Assessing the Seasonal Dynamics of Nitrate and Sulfate Aerosols at the South Pole Utilizing Stable Isotopes

Wendell Walters, Greg Michalski, J. Böhlke, Becky Alexander, Joël Savarino, Mark Thiemens

▶ **To cite this version:**

Wendell Walters, Greg Michalski, J. Böhlke, Becky Alexander, Joël Savarino, et al.. Assessing the Seasonal Dynamics of Nitrate and Sulfate Aerosols at the South Pole Utilizing Stable Isotopes. Journal of Geophysical Research: Atmospheres, 2019, 124 (14), pp.8161-8177. 10.1029/2019JD030517 . hal-04776429

HAL Id: hal-04776429
https://hal.science/hal-04776429v1

Submitted on 12 Nov 2024

HAL is a multi-disciplinary open access archive for the deposit and dissemination of scientific research documents, whether they are published or not. The documents may come from teaching and research institutions in France or abroad, or from public or private research centers.

L'archive ouverte pluridisciplinaire **HAL**, est destinée au dépôt et à la diffusion de documents scientifiques de niveau recherche, publiés ou non, émanant des établissements d'enseignement et de recherche français ou étrangers, des laboratoires publics ou privés.

Copyright

Check for updates

JGR Atmospheres

RESEARCH ARTICLE
10.1029/2019JD030517

Assessing the Seasonal Dynamics of Nitrate and Sulfate Aerosols at the South Pole Utilizing Stable Isotopes

Wendell W. Walters[1,2], Greg Michalski[3,4], J. K. Böhlke[5], Becky Alexander[6], Joël Savarino[7], and Mark H. Thiemens[8]

[1]Department of Earth, Environmental, and Planetary Sciences, Brown University, Providence, RI, USA, [2]Institute at Brown for Environment and Society, Brown University, Providence, RI, USA, [3]Department of Earth, Atmospheric, and Planetary Sciences, Purdue University, West Lafayette, IN, USA, [4]Department of Chemistry, Purdue University, West Lafayette, IN, USA, [5]U.S. Geological Survey, Reston, VA, USA, [6]Department of Atmospheric Sciences, University of Washington, Seattle, WA, USA, [7]Université Grenoble Alpes, CNRS, IRD, Grenoble INP, IGE, Grenoble, France, [8]Department of Chemistry and Biogeochemistry, University of California, San Diego, CA, USA

Key Points:
- The stable isotope compositions of nitrate and sulfate were measured from aerosol samples collected at the South Pole
- Distinct seasonal cycles were found in both concentration and isotopic compositions resulting from changing contributions of emission sources and oxidation chemistry
- The budgets of nitrate and sulfate at the South Pole are complex functions of transport, localized chemistry, biological activity, and meteorological conditions

Supporting Information:
- Supporting Information S1

Correspondence to:
W. W. Walters, and G. Michalski,
wendell_walters@brown.edu;
gmichals@purdue.edu

Citation:
Walters, W. W., Michalski, G., Böhlke, J. K., Alexander, B., Savarino, J., & Thiemens, M. H. (2019). Assessing the seasonal dynamics of nitrate and sulfate aerosols at the South Pole utilizing stable isotopes. *Journal of Geophysical Research: Atmospheres*, *124*, 8161–8177. https://doi.org/10.1029/2019JD030517

Received 20 FEB 2019
Accepted 23 JUN 2019
Accepted article online 6 JUL 2019
Published online 22 JUL 2019

©2019. American Geophysical Union. All Rights Reserved.

Abstract Atmospheric nitrate (NO_3^- = particulate NO_3^- + gas-phase nitric acid [HNO_3]) and sulfate (SO_4^{2-}) are key molecules that play important roles in numerous atmospheric processes. Here, the seasonal cycles of NO_3^- and total suspended particulate sulfate ($SO_4^{2-}{}_{(TSP)}$) were evaluated at the South Pole from aerosol samples collected weekly for approximately 10 months (26 January to 25 October) in 2002 and analyzed for their concentration and isotopic compositions. Aerosol NO_3^- was largely affected by snowpack emissions in which [NO_3^-] and $\delta^{15}N(NO_3^-)$ were highest (49.3 ± 21.4 ng/m^3, $n = 8$) and lowest (−47.0 ± 11.7‰, $n = 5$), respectively, during periods of sunlight in the interior of Antarctica. The seasonal cycle of $\Delta^{17}O(NO_3^-)$ reflected tropospheric chemistry year-round with lower values observed during sunlight periods and higher values observed during dark periods, reflecting shifts from HO_x- to O_3-dominated oxidation chemistry. $SO_4^{2-}{}_{(TSP)}$ concentrations were highest during austral summer and fall (86.7 ± 73.7 ng/m^3, $n = 18$) and are indicated to be derived from dimethyl sulfide (DMS) emissions, as $\delta^{34}S(SO_4^{2-})_{(TSP)}$ values (18.5 ± 1.0‰, $n = 10$) were similar to literature $\delta^{34}S$(DMS) values. The seasonal cycle of $\Delta^{17}O(SO_4^{2-})_{(TSP)}$ exhibited minima during austral summer (0.9 ± 0.1‰, $n = 5$) and maxima during austral fall (1.3 ± 0.3‰, $n = 6$) and austral spring (1.6 ± 0.1‰, $n = 5$), indicating a shift from HO_x- to O_3-dominated chemistry in the atmospheric derived SO_4^{2-} component. Overall, the budgets of NO_3^- and $SO_4^{2-}{}_{(TSP)}$ at the South Pole were complex functions of transport, localized chemistry, biological activity, and meteorological conditions, and these results will be important for interpretations of oxyanions in ice core records in the interior of Antarctica.

1. Introduction

The interior of Antarctica is a unique region to study atmospheric chemistry because of its pristine nature, distinctive climatology, and the potential influence of stratospheric dynamics on tropospheric chemistry (Hill-Falkenthal et al., 2013; McCabe et al., 2007; Savarino et al., 2007; Shaw, 1988; Wagenbach, 1996). The region is also vital for paleoclimatology studies that relate trace gases (e.g. carbon dioxide [CO_2], methane [CH_4], and nitrous oxide [N_2O]) and aerosols, trapped in the polar ice, to past global climate shifts and feedback mechanisms (Alexander et al., 2003; Augustin et al., 2004; Barnola et al., 1987; Legrand et al., 1988; Leuenberger et al., 1992; MacFarling Meure et al., 2006; Röthlisberger et al., 2000). By measuring changes in greenhouse gas concentrations and their stable isotopic compositions, it is possible to place constraints on the change in sources of these compounds over time (Craig et al., 1988; Friedli et al., 1986; Leuenberger et al., 1992). This is because these gases have small photochemical removal rates, which gives them a long atmospheric lifetime (~10–100 year). This allows them to be thoroughly mixed in the global troposphere and incorporated into the ice before removal mechanisms can induce any noticeable isotopic fractionation; thus, the change in isotopic composition can be related, by mass balance, to global source changes.

Interpreting the isotopic compositions of nitrate (NO_3^-) and sulfate (SO_4^{2-}) in ice is more complex because both the aerosol and gaseous components of these compounds have atmospheric lifetimes that are considerably shorter (days to weeks) relative to greenhouse gases. However, these are important oxyanions to study because of the substantial role they play in the chemical activity of the atmosphere with important

21698996, 2019, 14, Downloaded from https://agupubs.onlinelibrary.wiley.com/doi/10.1029/2019JD030517 by Cochrane France, Wiley Online Library on [11/11/2024]. See the Terms and Conditions (https://onlinelibrary.wiley.com/terms-and-conditions) on Wiley Online Library for rules of use; OA articles are governed by the applicable Creative Commons License

implications for climatic forcing and controls on the atmospheric oxidation budget (Arimoto et al., 2001; Hauglustaine et al., 2014; Haywood & Boucher, 2000; Kiehl et al., 2000). NO_3^- and SO_4^{2-} are formed as secondary products from the oxidation of precursor gases, nitrogen oxides (NO_x = NO + NO_2) and sulfur dioxide (SO_2). Primary sources of SO_4^{2-} also exist including direct emission via sea salt particles. Due to the conserved mass of sulfur (S) and nitrogen (N) between the precursor gases and the oxidized end-products of NO_3^- and of SO_4^{2-}, N ($\delta^{15}N$) and S ($\delta^{34}S$) isotopic compositions may serve as a proxy providing key information about emissions sources of reduced N and S gases (Hastings et al., 2009; Heaton, 1990; Nielsen, 1974). This may be a helpful tool to constrain N and S emissions sources that remain relatively unclear in the interior of Antarctica (Delmas, 2013; Legrand et al., 2017; Preunkert et al., 2008; Weller et al., 2018). In contrast, the oxygen (O) isotopic composition ($\delta^{18}O$ & $\Delta^{17}O$) is associated with the incorporation of oxygen atoms from various atmospheric oxidants, as gaseous precursors (i.e., NO_x and SO_2) are oxidized to NO_3^- or SO_4^{2-} (Alexander et al., 2005; Michalski et al., 2003). The number of isotopic studies of NO_3^- or SO_4^{2-} in polar regions are relatively meager but have received increased attention in recent years, and interpretations of the isotopic signals continue to evolve (Erbland et al., 2013; Frey et al., 2009; Hill-Falkenthal et al., 2013; Ishino et al., 2017; McCabe et al., 2007; Savarino et al., 2007, 2016). However, to utilize stable isotopes in NO_3^- and SO_4^{2-} in a paleoclimate context (i.e., ice core studies) in the interior of Antarctica, we must have a better understanding of the isotopic signatures of these molecules in the polar atmosphere.

Isotopic compositions of NO_3^- can be a useful way to understand sources and oxidation pathways responsible for its formation. Previous works in Antarctica have indicated snowpack photolysis and localized recycling, continental transport, and stratospheric inputs as important sources of NO_3^- (Savarino et al., 2007). Snowpack NO_3^- photolysis plays an important role in polar environments, initiating a rapid recycling of NO_3^- (i.e., snowpack loss as NO_x, oxidation, and deposition; Davis et al., 2008; Erbland et al., 2013; Frey et al., 2009), but does not represent a new source of NO_3^- to Antarctica. Long-range transport of continental- ($\delta^{15}N = 2.5\pm12.5‰$; Elliott et al., 2009; Freyer, 1978; Heaton, 1987) and stratospheric-sourced ($\delta^{15}N = 19\pm3‰$; Savarino et al., 2007) NO_3^- are isotopically distinct from locally recycled NO_3^- ($\delta^{15}N = {}^-32.7\pm8.4‰$; Savarino et al., 2007). ^{15}N depleted NO_3^- originating from snowpack photolysis is due to the large fractionation ($^{15}\varepsilon$~48‰; Berhanu et al., 2015; Berhanu et al., 2014), during photolysis in austral summer.

Oxidation pathways during NO_3^- formation may be evaluated using $\Delta^{17}O$ data (McCabe et al., 2007; Michalski et al., 2003; Morin et al., 2007, 2009; Savarino et al., 2007). During NO_x oxidation, O atoms of the responsible oxidants are incorporated into the product NO_3^-. Tropospheric ozone (O_3) has an elevated $\Delta^{17}O(O_{3bulk})$ near 26‰ (Johnston & Thiemens, 1997; Krankowsky et al., 1995; Vicars et al., 2012; Vicars & Savarino, 2014), with the transferrable O atom of O_3 associated with the terminal end of O_3 (O_{3term}) possessing a $\Delta^{17}O(O_{3term})$ of 39.3±2.0‰ (Vicars & Savarino, 2014). This contrasts with most other atmospheric O-bearing molecules including molecular oxygen (O_2), water (H_2O), and peroxy radicals (RO_2 or HO_2) that have $\Delta^{17}O$ values near 0‰ (Barkan & Luz, 2005). These differences provide quantitative measures to evaluate NO_x oxidation chemistry involving various contributions from O_3, HO_x, RO_x, and XO (where X = bromine [Br] or chlorine [Cl]) oxidation pathways (Michalski et al., 2003) and to compare modeled formation pathways (Alexander et al., 2009) with direct observations (Morin et al., 2008; Savarino et al., 2013). The $\Delta^{17}O$ observed in NO_3^- is a balance between the $\Delta^{17}O$ of NO_2 and the subsequent oxidation pathway resulting in NO_3^-. The $\Delta^{17}O$ of NO_2 should reflect NO_x photochemical cycling between NO-O_3-RO_2 (or HO_2), resulting in expected values near 28‰ to 39‰ (Morin et al., 2011), representing a NO + O_3 branching ratio of 0.72 to 1.0. Post-NO_2 reaction pathways have been assumed to reflect O isotopic mass balance with the associated oxidants, which has been derived in previous works (Alexander et al., 2009; Ishino et al., 2017; Michalski et al., 2003; Morin et al., 2009). Based on this framework, the NO_2 + OH pathway is expected to produce the lowest $\Delta^{17}O(NO_3^-)$ values (17.3‰ to 25.1‰), while volatile organic compound (VOC) hydrogen abstraction by the nitrate radical (NO_3 + VOC) and $XONO_2$ hydrolysis are expected to produce the highest $\Delta^{17}O(NO_3^-)$ values (38.0‰ to 42.3‰) (Table 1; Morin et al., 2011). Thus, $\Delta^{17}O(NO_3^-)$ may be useful to further understand oxidation chemistry involving NO_3^- in sensitive polar environments.

Previous studies have indicated marine biogenic sulfur, sea salt, continental transport (i.e., derived from mineral, continental biogenic, and anthropogenic sources) and stratospheric inputs to be important SO_4^{2-} sources to the interior of Antarctica (Arimoto et al., 2001; Hill-Falkenthal et al., 2013). These sources

Table 1
Summary of NO_3^- and SO_4^{2-} Oxidation Pathways and Their Expected $\Delta^{17}O$ Values (Adapted From Ishino et al., 2017)

Species	Oxidation pathway	$\Delta^{17}O$(oxidant)(‰)	Transferring factor	$\Delta^{17}O$ product(‰)
NO_3^-	NO_2 + OH	0 (OH)	2/3(NO_2)	17.3–25.1
	N_2O_5 hydrolysis	(37.3–42.3) (O_{3term}), 0 (H_2O)	2/3(NO_2) + 1/6(O_{3term})	31.0–35.2
	NO_3 + VOC	(37.3–42.3) (O_{3term})	2/3(NO_2) + 1/3(O_{3term})	38.0–42.3
	$XONO_2$ hydrolysis	(37.3–42.3) (BrO)	2/3(NO_2) + 1/3(BrO)	38.0–42.3
SO_4^{2-}	SO_2 + OH	0 (OH)	0	0
	SO_3^{2-} + $O_{3(aq)}$	37.3–42.3 (O_{3term})	1/4(O_{3term})	9.3–10.6
	HSO_3^- + $H_2O_{2\ (aq)}$	1.6 (H_2O_2)	1/2(H_2O_2)	0.8
	SO_3^{2-} + O_2(cat. Fe, Mn)	−0.3 (O_2)	1/4(O_2)	−0.1
	SO_3^{2-} + HOX + H_2O	37.3–42.3 (HOX)	—	0

Note. $\Delta^{17}O$ values of NO_3^- are estimated based on box model results of Morin et al. (2011). $\Delta^{17}O$ values of SO_4^{2-} are adapted based on calculations from Savarino et al. (2000).

have reported $\delta^{34}S$ signatures of 18.6±1.9‰ for dimethyl sulfide (DMS; Patris et al., 2002; Sanusi et al., 2006), 21±0.1‰ for sea salt SO_4^{2-} (Rees et al., 1978), 3±3‰ for continental SO_4^{2-} (Jenkins & Bao, 2006; Li & Barrie, 1993; Norman et al., 1999), and 2.6±0.3‰ for stratospheric SO_4^{2-} (Castleman et al., 1974), respectively. These relatively distinctive $\delta^{34}S$ source signatures offer the possibility to constrain the SO_4^{2-} budget in the interior of Antarctica.

$\Delta^{17}O$ analysis of SO_4^{2-} is a well-established tool for assessing SO_2 oxidation pathways (Alexander et al., 2005; Jenkins & Bao, 2006; Lee & Thiemens, 2001; Savarino et al., 2000). Atmospheric SO_2 rapidly attains isotopic equilibrium with H_2O (Holt et al., 1981). Thus, any $\Delta^{17}O$ signature observed in SO_4^{2-} derives from SO_2 oxidation and can be used to assess the relative importance of SO_2 oxidation pathways, allowing for an understanding of the relative importance of aqueous-phase and gas-phase oxidation (Alexander et al., 2005, 2009; Dominguez et al., 2008; Hill-Falkenthal et al., 2013; Lee & Thiemens, 2001; Savarino et al., 2003). Gas-phase oxidation via OH will result in a $\Delta^{17}O(SO_4^{2-})$ of 0‰ when isotopic equilibrium with H_2O is reached. Previous works have shown that the $\Delta^{17}O$ signature of $O_{3(bulk)}$ (26‰; Vicars & Savarino, 2014) and hydrogen peroxide (~1.7‰; Lyons, 2001; Savarino & Thiemens, 1999) are partially transferred into SO_4^{2-} based on O mass balance resulting in $\Delta^{17}O(SO_4^{2-})$ values near 6.5‰ and 0.8‰, respectively. However, we note that if O atom transfer occurs from $O_{3(term)}$ as indicated by *ab initio* results (Liu et al., 2001), then the S (IV) (=$SO_2{\cdot}H_2O$ + HSO_3^- + SO_3^{2-}) + O_3 oxidation pathway could have a $\Delta^{17}O$ as high as 9.3–10.6‰ (Table 1). Other potentially important aqueous-phase S (IV) oxidation pathways include aqueous metal-catalyzed O_2 oxidation, which results in estimated $\Delta^{17}O(SO_4^{2-})$ of −0.1‰ (Barkan & Luz, 2005) and S (IV) oxidation via hypohalous acids (HOX = HOBr + HOCl) with an expected $\Delta^{17}O(SO_4^{2-})$ of 0‰ due to rapid equilibrium with H_2O (Chen et al., 2016; Fogelman et al., 1989; Troy & Margerum, 1991). Tropospheric S (IV) oxidation via O_3 is the only mechanism producing SO_4^{2-} with $\Delta^{17}O$ values >1‰, allowing for quantitative evaluation of the relative contribution of O_3 during SO_4^{2-} formation (Table 1). Aqueous-phase formation of SO_4^{2-} is highly dependent upon pH, liquid water content, and availability of oxidants (Pandis & Seinfeld, 1989). The O_3 oxidation pathway is important primarily when the liquid water content is large, and the solution pH is above 5 (Liang & Jacobson, 1999). Therefore, $\Delta^{17}O(SO_4^{2-})$ can provide useful observational constraints on the oxidation dynamics involving S(IV).

Previous isotopic studies have reported the $\Delta^{17}O(NO_3^-)$ at the coast of Antarctica (Ishino et al., 2017; Savarino et al., 2007) and in the interior of Antarctica (Erbland et al., 2013; Frey et al., 2009; McCabe et al., 2007; Savarino et al., 2016), generally finding a distinctive $\Delta^{17}O$ seasonal cycle that reflects the higher relative contribution of O_3 oxidation and/or stratospheric input during the austral winter and increased HO_x + RO_x oxidation during the austral summer. Previous Antarctica $\delta^{15}N(NO_3^-)$ measurements indicate a distinctive seasonal cycle driven by localized snowpack emissions during periods of sunlight (Erbland et al., 2013; Frey et al., 2009; Savarino et al., 2007). Studies of $\Delta^{17}O(SO_4^{2-})$ at Dumont d'Urville (DDU; Ishino et al., 2017) and Dome C (Hill-Falkenthal et al., 2013) also indicate seasonal cycles reflecting shifts in gas-phase to aqueous-phase oxidation (Hill-Falkenthal et al., 2013). However, the oxidation dynamics involving NO_3^- and SO_4^{2-} over Antarctica, particularly in the interior, are far from solved (Hill-Falkenthal et al., 2013;

21698996, 2019, 14, Downloaded from https://agupubs.onlinelibrary.wiley.com/doi/10.1029/2019JD030517 by Cochrane France, Wiley Online Library on [11/11/2024]. See the Terms and Conditions (https://onlinelibrary.wiley.com/terms-and-conditions) on Wiley Online Library for rules of use; OA articles are governed by the applicable Creative Commons License

21698996, 2019, 14, Downloaded from https://agupubs.onlinelibrary.wiley.com/doi/10.1029/2019JD030517 by Cochrane France, Wiley Online Library on [11/11/2024]. See the Terms and Conditions (https://onlinelibrary.wiley.com/terms-and-conditions) on Wiley Online Library for rules of use; OA articles are governed by the applicable Creative Commons License

Savarino et al., 2016). Additionally, $\Delta^{17}O(SO_4^{2-})$ from snow pit samples at the South Pole has recently been shown to have large interannual variation related to El Nino Southern Oscillations events (Shaheen et al., 2013). To improve understanding of the dynamics associated with NO_3^- and SO_4^{2-} aerosols in the interior of Antarctica, here we present concentration and $\delta^{15}N$, $\delta^{34}S$, $\delta^{18}O$, and $\Delta^{17}O$ measurements of atmospheric NO_3^- and total suspended particulate SO_4^{2-} ($SO_4^{2-}{}_{(TSP)}$) collected at the South Pole for approximately 10 months in 2002. The dynamics of NO_3^- and $SO_4^{2-}{}_{(TSP)}$ are assessed in terms of source changes ($\delta^{15}N$ and $\delta^{34}S$) and oxidation chemistry ($\Delta^{17}O$ & $\delta^{18}O$). These data will be useful for understanding the seasonal cycling of NO_3^- and $SO_4^{2-}{}_{(TSP)}$ concentrations in the atmosphere at the South Pole, which is unique in lacking a diurnal solar radiation cycle, in contrast to Dome C or coastal Antarctic sites.

2. Materials and Methods

2.1. South Pole Atmospheric Conditions

Antarctica has a unique climate and meteorology that has important implications for atmospheric chemistry as previously well described (Davis et al., 2004; Helmig et al., 2007; Hill-Falkenthal et al., 2013; Legrand et al., 2009; Stohl & Sodemann, 2010; Wendler & Kodama, 1984). The South Pole is 2,836 m above sea level on the interior high plateau, from which the continent slopes downward toward its perimeter (Wendler & Kodama, 1984). There are 6 months of continuous sunlight and 6 months without sunlight. This cycle in sunlight can have a strong influence on chemistry driven by photolysis, in which these reactions shut down during the austral winter and can play an important role on localized concentrations of atmospheric oxidants that are often driven by photolysis reactions. Solar radiation is similar during both austral spring and fall; however, due to the buildup of photolabile molecules during the austral winter, solar radiation returning in the austral spring can create a different chemical environment in comparison to austral fall. In addition, greater amounts of UV radiation reach the troposphere during the austral spring due to the annual occurrence of stratospheric O_3 depletion during the early austral spring. The 2002 O_3 hole was relatively small compared to the previous 6 years and split into two holes at the end of September due to the appearance of sudden stratospheric warming (Varotsos, 2002). Data from the South Pole Station Meteorology Office (http://amrc.ssec.wisc.edu/usap/southpole/) indicate (1) South Pole surface temperatures have a typical annual range between −76 and −18 °C with a mean annual temperature of −49.5 °C, (2) there are strong surface inversions especially during the austral winter, (3) there is generally very little precipitation in Antarctica's interior and the majority consists of ice crystals or diamond dust, and (4) winds are generally light compared to the coastal regions of Antarctica, and the prevailing direction is from grid north.

2.2. Aerosol Collection

Aerosols were collected on precleaned 20.3 × 25.4 cm glass fiber filters fitted onto a high-volume air sampler from 26 January to 25 October in 2002. The glass fiber filter is assumed to collect total atmospheric nitrate (aerosol NO_3^- and $HNO_{3(g)}$) as previously suggested (Frey et al., 2009). The sampler was located on the roof of the Atmospheric Research Observatory (elevation ~2,850 m), which is in the designated clean air sector roughly 1 km upwind of the South Pole Observatory (SPO; 90.00°S, 59.00°E). The clean upwind air is expected to be representative of the true mixed background atmosphere over Antarctica with minimal influence from anthropogenic contamination from the station. Aerosols were collected for 7-day periods with a flow rate of 1 m^3/min at standard temperature and pressure, yielding an average pumped air volume of 10,080 m^3 per collected sample. Filters were kept frozen after collection and during shipment to University of California San Diego for subsequent chemical and isotopic analysis.

2.3. Anion Concentrations and Isotopic Characterization

Water-soluble aerosol compounds were extracted from the filters using 100 ml of Millipore water and mechanical shaking for 10 min. Filter extracts were analyzed for NO_3^-, and SO_4^{2-} concentrations by ion chromatography (Dionex 2020i). Filter NO_3^- and SO_4^{2-} blanks never exceeded 2% of the sample; thus, blank corrections were neglected for these species. Based on the concentrations, multiple filters were combined by date to ensure ~8 μmol of NO_3^- and SO_4^{2-} were available for isotopic analysis. Typically, sea salt SO_4^{2-} ($ss\text{-}SO_4^{2-}$) contribution in a sample can be calculated by assuming it is the source of sodium (Na^+) with the ratio of SO_4^{2-} to Na^+ in sea water (i.e., $(SO_4^{2-}/Na^+)_{sea\ salt}$ ~ 0.25) and the non-sea salt SO_4^{2-}

21698996, 2019, 14, Downloaded from https://agupubs.onlinelibrary.wiley.com/doi/10.1029/2019JD030517 by Cochrane France, Wiley Online Library on [11/11/2024]. See the Terms and Conditions (https://onlinelibrary.wiley.com/terms-and-conditions) on Wiley Online Library for rules of use; OA articles are governed by the applicable Creative Commons License

(nss-SO_4^{2-}) contribution can be determined by difference (nss-SO_4^{2-} = $[SO_4^{2-}]_{(TSP)}$ − [ss-SO_4^{2-}]; e.g., Patris et al., 2000). However, adjustments for ss-SO_4^{2-} were not made in the current study because of high and variable Na^+ filter blanks. Previous aerosol SO_4^{2-} measurements in the interior of Antarctica (Dome C) have indicated a relative minor contribution from sea salt SO_4^{2-} of 3.9 to 6.7% during the austral summer (15 January to 15 March 2010) with an increasing relative contribution during austral winter of 31.7% to 33.6% (15 May to 15 August 2010; Hill-Falkenthal et al., 2013). We report $SO_4^{2-}{}_{(TSP)}$ (sea salt + secondary SO_4^{2-}) and note that the sea salt SO_4^{2-} contribution is expected to be relatively small, particularly during the austral summer, but somewhat higher during austral winter.

The O isotope ratios of NO_3^- and SO_4^{2-} were determined using the thermal decomposition method (Michalski et al., 2002; Savarino et al., 2001). Briefly, the filter extracts were pumped into a high-capacity anion trapping column (Dionex AG15) that was attached to the injection valve of a Dionex 2020i ion chromatograph, equipped with an anion analytical column (AS9-HC) and an H^+ suppressor membrane column. A 260-mM sodium hydroxide eluent solution was diluted 1:30 with Millipore water and flowed through the system at 0.8 ml/min. Peaks were detected by an online conductivity detector. Three distinct peaks were eluted over a 30-min separation period representing organic/methanesulfonic acid (MSA)/Cl^- (14 min), NO_3^- (23 min), and SO_4^{2-} (30 min). Owing to the H^+ suppressor membrane column, the sample ions left the system in their acid forms while the hydroxide eluent was neutralized. The separated H_2SO_4 and HNO_3 were further processed through an off-line cation exchange membrane in silver (Ag^+) form to generate silver nitrate ($AgNO_3$) and silver sulfate (Ag_2SO_4) solutions (10 ml) that were then freeze dried. The silver salts were rehydrated with 70 μl of Millipore water and pipetted into silver boats or precombusted quartz boats, which were then freeze dried. The $AgNO_3$ and Ag_2SO_4 were then thermally decomposed to evolve O_2 gas that was then analyzed by a dual-inlet isotope ratio mass spectrometer (IRMS). Based on standards of the same size that were processed in a similar manner, the precision of the analysis is ±0.2‰ for $\Delta^{17}O$ and ±2.0‰ for $\delta^{18}O$ for both NO_3^- and SO_4^{2-}. Sample O isotopic data was normalized to reference materials as previously described (Michalski et al., 2002; Savarino et al., 2001).

During the thermal decomposition of the silver salts, liquid nitrogen traps cryogenically removed the product gases, $NO_{2(g)}$ and $SO_{2(g)}$ (Michalski et al., 2002; Savarino et al., 2001). The $NO_{2(g)}$ aliquots were cryogenically transferred to evacuated glass tubes that were flame sealed and sent to the U.S. Geological Survey (USGS) in Reston, Virginia, for $\delta^{15}N$ analysis. Additional aliquots of $NO_{2(g)}$ produced from the nitrate isotopic reference material USGS35 were prepared similarly but at a later date. At USGS, sealed tubes containing $NO_{2(g)}$ were cracked under vacuum, and the NO_2 was transferred cryogenically with liquid N_2 to quartz glass tubes containing copper (Cu), copper(I) oxide (Cu_2O), and calcium oxide (CaO), which were then flame sealed and baked at 850 °C and cooled slowly to convert $NO_{2(g)}$ to N_2 and remove traces of H_2O and CO_2 (Böhlke et al., 1993). The baked tubes were cracked under vacuum at the inlet to a dual-inlet IRMS, and the N_2 was analyzed against aliquots of N_2 prepared directly from nitrate isotopic reference materials RSIL-N55 (+3.6‰) and USGS32 (+180‰) with reproducibility of ±0.1% to 0.2‰. Overall $\delta^{15}N$ uncertainties may have been larger because of potential fractionation effects caused by incomplete NO_2 production and (or) cryogenic trapping, as N yields were calculated to range from 45% to 103% with an average of 62±18‰ ($n = 9$; Table S1 in the supporting information). NO_2 aliquots generated from USGS35 a year later had substantially lower yields relative to the amount of thermal decomposed NO_3^- (16% to 29%) and low apparent $\delta^{15}N$ (−14.0 ± 0.1‰), compared to the reported reference value of +2.7‰. If this apparent $\delta^{15}N$ offset was caused by fractionation that was related to N yield, and that also affected the samples analyzed earlier, then it is possible the apparent sample $\delta^{15}N$ values were too low by varying amounts on the order of 0 to 8‰. Nonetheless, there was only a weak correlation between $\delta^{15}N$ and N yield among the samples (coefficient of variation [R^2] = 0.19), and the range of values was large and exhibited a strong seasonal pattern (see section 3.2.1) that was independent of yield. Residual $SO_{2(g)}$ from thermal decomposition was oxidized to SO_4^{2-} using a 30% hydrogen peroxide solution and precipitated as barium sulfate ($BaSO_4$). The $BaSO_4$ was mixed with vanadium oxide (V_2O_5), and $\delta^{34}S$ was determined using an elemental analyzer interface and continuous flow IRMS, with standard deviations of approximately ±0.3‰, based on replicate analysis of international standard reference materials.

All isotopic compositions are reported relative to reference standards using delta (δ) notation in units of per mil (‰; equation (1)):

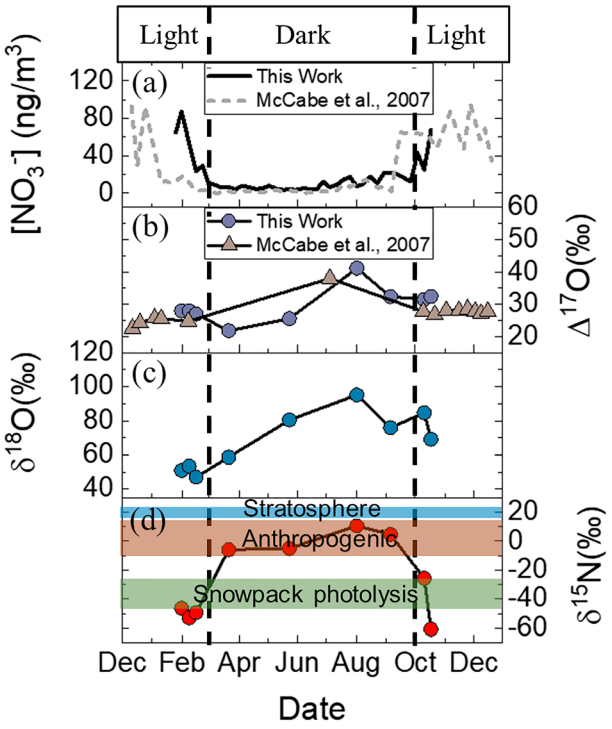

Figure 1. Seasonal variation of atmospheric NO_3^- collected at the South Pole in 2002 including (a) concentrations, (b) $\Delta^{17}O(NO_3^-)$, (c) $\delta^{18}O(NO_3^-)$, and (d) $\delta^{15}N(NO_3^-)$. A comparison between previously reported NO_3^- concentrations and $\Delta^{17}O$ from aerosols collected at the South Pole (12/1/03 to 12/01/04) is shown in a and b (McCabe et al., 2007). Ranges of potential $\delta^{15}N$ (NO_3^-) sources are indicated in d, including stratospheric inputs (19±3‰; Savarino et al., 2007), long-range transport of continental NO_3^- derived from anthropogenic emissions (2.5±12.5‰; Elliott et al., 2009; Freyer, 1978; Heaton, 1987), and localized recycling of NO_3^- during periods of snowpack photolysis (−32.7±8.4‰; Savarino et al., 2007). Periods of constant sunlight and darkness at the South Pole are separated by the black dashed lines. Isotopic data for composite samples are plotted at the collection starting point (Table 2).

$$\delta(‰) = 1000\left(\frac{R_{samp}}{R_{ref}} - 1\right), \quad (1)$$

where R refers to the ratio of the heavy to the light isotope (i.e., $^{15}N/^{14}N$, $^{34}S/^{32}S$, $^{17}O/^{16}O$, and $^{18}O/^{16}O$) for the sample or reference, respectively. Atmospheric nitrogen (N_2), Vienna Cañon Diablo troilite, and Vienna Standard Mean Ocean Water are the established international delta-scale references for N, S, and O, respectively. Oxygen isotope mass-independence ($\Delta^{17}O$) was quantified using the linear definition with a mass-dependent coefficient of 0.52, which is approximately representative of O mass-dependent coefficients expected and observed in nature (equation (2)):

$$\Delta^{17}O = \delta^{17}O - 0.52 \times \delta^{18}O. \quad (2)$$

We note that the exact O mass-dependent coefficient will depend on specific equilibrium or kinetic processes, which will have different $\ln(1 + \delta^{17}O)$ versus $\ln(1 + \delta^{18}O)$ relations with slopes between 0.5 and 0.531 (Young et al., 2002). However, a coefficient of 0.52 was chosen to be consistent with similar previously published works (Alexander et al., 2004; Michalski et al., 2003; Morin et al., 2007; Savarino et al., 2007) and because it represents a reasonable average of O mass-dependent coefficients expected and observed in nature (Barkan & Luz, 2003; Kaiser et al., 2004; Weston, 2006).

2.4. Complementary Analysis

Air mass back trajectories arriving at the South Pole were analyzed using National Oceanic and Atmospheric Administration's HYSPLIT model (Stein et al., 2015). The model was initiated using the National Center for Environmental Prediction and the National Center for Atmospheric Research global reanalysis data archive meteorology in a regular 2.5° × 2.5° longitude-latitude grid. The 7-day backward trajectories were computed for air masses arriving at the South Pole at an altitude of 3,000 m above sea level every 5 days for the entire sampling period (26 January to 25 October 2002). The tropospheric lifetimes of NO_3^- and SO_4^{2-} typically are on the order of a few days up to a couple of weeks in the free troposphere (Adams et al., 1999; Levy et al., 1999). However, trajectories tend to become increasingly uncertain the further back in time they are used. A duration of 7 days was chosen as a balance between higher certainty and the expected atmospheric lifetime of NO_3^- and SO_4^{2-} aerosols. Ancillary data including temperature, relative humidity, solar irradiance, and [O_3] data for 2002 were obtained from the SPO (National Oceanic and Atmospheric Administration; https://www.esrl.noaa.gov/gmd/dv/data/index.php?site=SPO) and used for statistical analysis.

3. Results

3.1. Concentrations

Weekly measured [NO_3^-] and $[SO_4^{2-}]_{(TSP)}$ in 2002 are displayed in Figures 1 and 2, respectively. Overall, [NO_3^-] and $[SO_4^{2-}]_{(TSP)}$ ranged from 3.6 to 87.2 ng/m^3 and 6.5 to 266.3 ng/m^3, respectively. Linear regression correlations between measured concentrations and reported ancillary data (averaged over 1-week aerosol collection periods) were reported separately for [NO_3^-] and $[SO_4^{2-}]_{(TSP)}$ as correlation matrices in the supporting information (Tables S2 and S3). Overall, a strong positive correlation was found between [NO_3^-] and solar irradiance ($R^2 = 0.59$), while the temperature was positively correlated with $[SO_4^{2-}]_{(TSP)}$ ($R^2 = 0.67$; Tables S2 and S3). Temporal analyses of [NO_3^-] and $[SO_4^{2-}]_{(TSP)}$ indicated similar seasonal cycles, in which concentrations were generally highest during the austral summer and lowest during

21698996, 2019, 14, Downloaded from https://agupubs.onlinelibrary.wiley.com/doi/10.1029/2019JD030517 by Cochrane France, Wiley Online Library on [11/11/2024]. See the Terms and Conditions (https://onlinelibrary.wiley.com/terms-and-conditions) on Wiley Online Library for rules of use; OA articles are governed by the applicable Creative Commons License

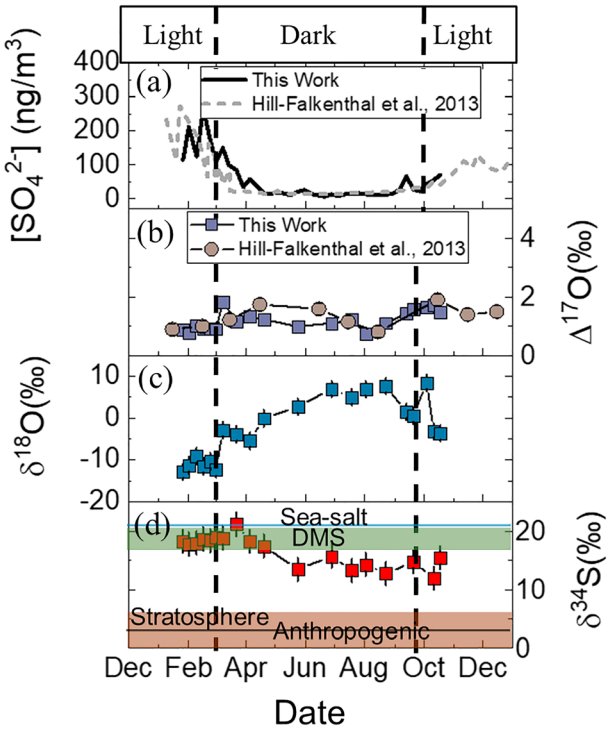

Figure 2. Seasonal variations of atmospheric $SO_4^{2-}{}_{(TSP)}$ collected from aerosols in 2002 at the South Pole including (a) concentrations, (b) $\Delta^{17}O(SO_4^{2-}{}_{(TSP)})$, (c) $\delta^{18}O(SO_4^{2-}{}_{(TSP)})$, and (d) $\delta^{34}S(SO_4^{2-}{}_{(TSP)})$. A comparison between previously reported $SO_4^{2-}{}_{(TSP)}$ concentrations and $\Delta^{17}O(SO_4^{2-}{}_{(TSP)})$ from aerosols collected at Dome C (2010) is shown in a and b (Hill-Falkenthal et al., 2013). Ranges of typical $\delta^{34}S(SO_4^{2-})$ sources are indicated in d, including sea salt SO_4^{2-} (21±0.1‰; Rees et al., 1978), dimethyl sulfide (DMS; 18.6±1.9‰; Patris et al., 2002; Sanusi et al., 2006), continental SO_4^{2-} (3±3‰; Jenkins & Bao, 2006; Li & Barrie, 1993; Norman et al., 1999), and stratospheric SO_4^{2-} inputs (2.6±0.3‰; Castleman Jr et al., 1974). Periods of constant sunlight and darkness at the South Pole are separated by the black dashed lines. Isotopic data for composite samples are plotted at the collection starting point (Table 3).

austral winter (Figures 1 and 2). However, because $[NO_3^-]$ and $[SO_4^{2-}]_{(TSP)}$ were not strongly correlated (R^2 = 0.29), we present their results separately. The 7-day back trajectory analysis indicated that SP air masses derived from the interior of Antarctica (Figure 3). Slight seasonal variations were observed in which some austral fall (April to July) and austral winter (July to October) air masses traveled over the northern coastal regions of Antarctica before arriving at SPO, while air masses in austral summer (January to April) and austral spring (October to sampling end [25 October 2002]) circulated entirely over the interior of Antarctica (Figure 3). The back trajectories indicated that the air masses traveled almost entirely at an elevated altitude (generally above 2,500 m above sea level) before arriving at the South Pole (representative trajectories are provided in Figure S1).

3.1.1. $[NO_3^-]$

At the beginning of the year (January to March), $[NO_3^-]$ reached a maximum concentration of 86.2 ng/m^3 in late January and then decreased rapidly to a baseline concentration of approximately 5.0 ng/m^3 in early March. This strong decline in $[NO_3^-]$ overlapped with decreasing local solar irradiance. The background $[NO_3^-]$ was maintained until early July, after which $[NO_3^-]$ concentrations slowly increased until the end of the sampling period (25 October 2002). The observed seasonal pattern in $[NO_3^-]$ is similar to that previously reported for atmospheric NO_3^- collected at the South Pole (McCabe et al., 2007), Dome C (Erbland et al., 2013; Frey et al., 2009), and along the coast of Antarctica at DDU (Ishino et al., 2017; Savarino et al., 2007). The peak in $[NO_3^-]$ at the South Pole was previously observed to occur in early January (McCabe et al., 2007), while our record indicated a peak in early February (Figure 1). We note that our record does not represent a complete yearlong study and samples were not collected during early January. Possible differences in the peak $[NO_3^-]$ observed at the South Pole are therefore difficult to compare between these two records.

3.1.2. $[SO_4^{2-}]_{(TSP)}$

At the beginning of the year, $[SO_4^{2-}]_{(TSP)}$ was relatively elevated and reached a maximum of 211.4 ng/m^3 during mid-February and then slowly decreased to a baseline value of approximately 15 ng/m^3 in late April. This baseline $[SO_4^{2-}]_{(TSP)}$ concentration was maintained until mid-September. Subsequently, $[SO_4^{2-}]_{(TSP)}$ increased slightly and reached a value of 67.5 ng/m^3 in the final sample (25 October 2002). The observed $[SO_4^{2-}]$ seasonal cycle was consistent with previously reported measurements at Dome C (Hill-Falkenthal et al., 2013) and at DDU (Ishino et al., 2017).

3.2. Isotopic Compositions

3.2.1. Nitrate

Nine measurements of the isotopic composition of NO_3^- were made from the collected samples and are summarized in Table 2 with SPO data (https://www.esrl.noaa.gov/gmd/dv/data/index.php?site=SPO). We note that often several filters were combined to provide enough material (~8 μmol) for isotopic analysis (Table 2), resulting in relatively coarse seasonal resolution, particularly during austral winter when $[NO_3^-]$ was low. The $\delta^{15}N(NO_3^-)$ values ranged from −60.8‰ to 10.5‰ (Figure 1), approximately consistent with previous $\delta^{15}N$ measurements of NO_3^- collected in coastal Antarctica that ranged from −46.9‰ to 10.8‰ (Savarino et al., 2007) and at Dome C that ranged from −35‰ to 13‰ (Frey et al., 2009), which generally fell within the ranges of the expected NO_3^- sources including snowpack photolysis and localized recycling (−32.7±8.4‰; Savarino et al., 2007), long-range transport of continental NO_3^- (2.5±12.5‰; Elliott et al., 2009; Freyer, 1978; Heaton, 1987), and stratospheric inputs (estimated 19±3‰; Savarino et al., 2007; Figure 1). Multifactorial analysis indicated negative correlations between $\delta^{15}N$ and $[NO_3^-]$ (R^2 = 0.59) and solar

21698996, 2019, 14, Downloaded from https://agupubs.onlinelibrary.wiley.com/doi/10.1029/2019JD030517 by Cochrane France, Wiley Online Library on [11/11/2024]. See the Terms and Conditions (https://onlinelibrary.wiley.com/terms-and-conditions) on Wiley Online Library for rules of use; OA articles are governed by the applicable Creative Commons License

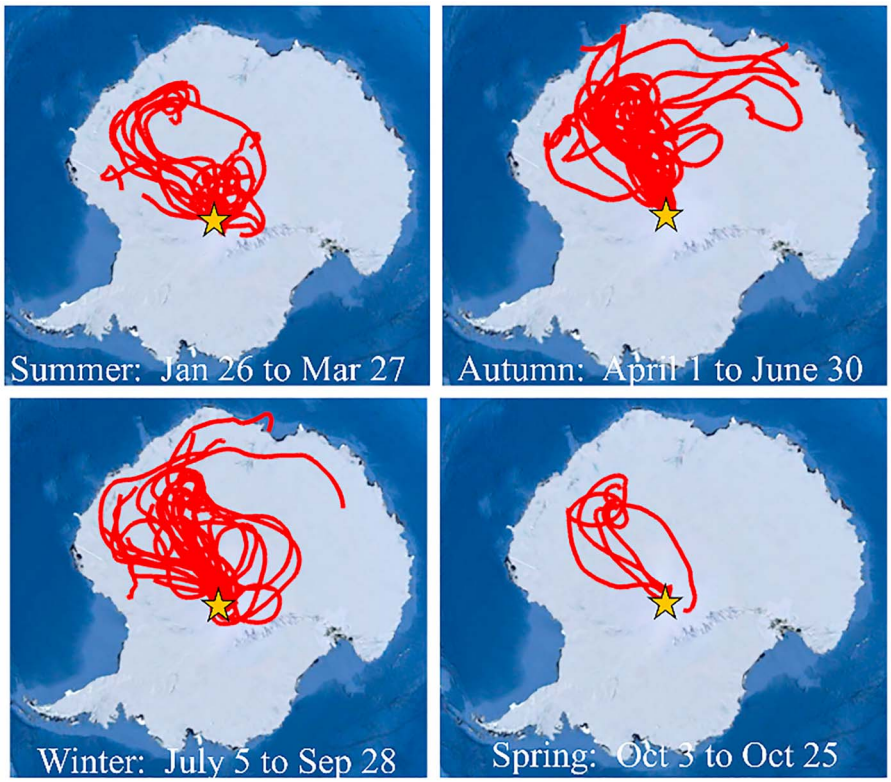

Figure 3. Hybrid Single-Particle Lagrangian Integrated Trajectory 7-day back trajectory analysis at the South Pole Observatory (90.00°S, 59.00°E; indicated by a star) for our sampling period of 26 January to 25 October 2002 and sorted by season. Maps are oriented grid north (prime meridian) in the upward direction.

irradiance ($R^2 = 0.55$) (Table S2). These correlations likely explain the $\delta^{15}N(NO_3^-)$ seasonal cycle observed in Figure 1, in which the lowest $\delta^{15}N(NO_3^-)$ values occurred during periods of sunlight, indicating the importance of snowpack emissions and localized photochemical recycling, while highest $\delta^{15}N(NO_3^-)$ occurred during periods of darkness (Figure 1). This pattern was similar to the seasonal variability previously reported at the coast (Savarino et al., 2007) and in the interior of Antarctica (Erbland et al., 2013; Frey et al., 2009).

Large variability was observed in $\delta^{18}O(NO_3^-)$ and $\Delta^{17}O(NO_3^-)$ that ranged from 47.0‰ to 95.1‰ and 21.8‰ to 41.1‰, respectively (Figure 1). These values were consistent with previously reported NO_3^-

Table 2
Summary of Average $[NO_3^-]$ (at STP), Temperature (Temp), Relative Humidity (RH), Solar Radiation, and $[O_3]$, for Each Collection Period Corresponding to NO_3^- Isotopic Composition Measurement (See Text for Details)

Collection date	Avg $[NO_3^-]$ (ng/m^3)	Temp (°C)[a]	RH(%)[a]	Solar Irradiance (W/m^2)[a]	$[O_3]$ (ppb$_v$)[a]	$\delta^{15}N(\pm0.2‰)$[b]	$\delta^{18}O(\pm2‰)$	$\Delta^{17}O(\pm0.2‰)$
02/01-02/09 (1)	87.2	−37.2±0.9	66.6±1.7	305.9±35.9	22.1±3.4	−46.3	51.0	27.9
02/09-02/16 (1)	53.0	−37.9±3.1	70.6±5.7	228.9±46.9	20.9±1.1	−53.0	53.5	28.0
02/16-02/23 (1)	24.0	−41.1±6.9	69.1±5.3	184.3±32.9	20.2±1.1	−49.4	47.0	26.9
03/22-04/19 (4)	5.9	−51.6±9.8	66.2±5.8	0.2±1.1	23.3±1.2	−5.9	58.7	21.8
05/24-06/28 (5)	5.9	−59.4±8.7	64.1±6.0	0±0	32.3±1.1	−5.1	80.4	25.6
08/02-08/23 (3)	11.7	−55.7±10.0	65.2±6.1	0±0	34.5±1.3	10.5	95.1	41.1
09/06-09/20 (2)	21.2	−57.3±6.8	63.4±3.9	0.1±1.0	33.1±1.1	4.6	75.9	32.3
10/11-10/18 (1)	25.3	−55.1±1.8	64.2±2.6	27.1±57.9	30.9±1.3	−25.7	84.6	31.4
10/18-10/25 (1)	67.6	−48.3±2.8	69.7±3.3	65.7±79.0	31.4±0.8	−60.8	69.0	32.4

Note. Parentheses indicate the number of weekly collected filter samples combined for isotopic analysis.
[a]Data obtained from the South Pole Observatory (NOAA; https://www.esrl.noaa.gov/gmd/dv/data/index.php?site=SPO); reported as $\bar{x}\pm1\sigma$ for the specified collection period. [b]See section 2.3 for discussion of $\delta^{15}N$ uncertainties.

21698996, 2019, 14, Downloaded from https://agupubs.onlinelibrary.wiley.com/doi/10.1029/2019JD030517 by Cochrane France, Wiley Online Library on [11/11/2024]. See the Terms and Conditions (https://onlinelibrary.wiley.com/terms-and-conditions) on Wiley Online Library for rules of use; OA articles are governed by the applicable Creative Commons License

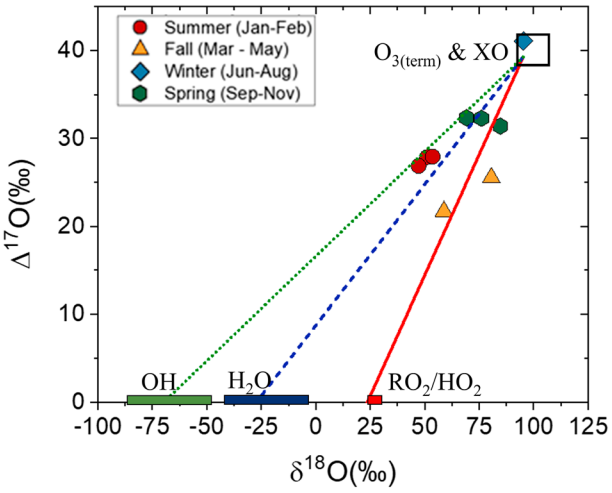

Figure 4. Relations between $\delta^{18}O$ and $\Delta^{17}O$ for collected NO_3^- sorted by season displayed with the high $\delta^{18}O$-$\Delta^{17}O$ end-member, $O_{3(term.)}$/XO (indicated by the black rectangle; $\delta^{18}O$ = 95–115‰; Johnston & Thiemens, 1997; and $\Delta^{17}O$ = 39.3‰; Vicars & Savarino, 2014) and its mixing relations with other important tropospheric O bearing atmospheric molecules including RO_2/HO_2 ($\delta^{18}O$ ~ 23.5‰ and $\Delta^{17}O$ ~ 0‰), H_2O ($\delta^{18}O$ = −40‰ and $\Delta^{17}O$ = 0‰, and OH ($\delta^{18}O$ = −80‰ and $\Delta^{17}O$ = 0‰; Michalski et al., 2012).

measurements in coastal Antarctica that ranged from 60‰ to 111‰ and 20.0‰ to 43.1‰ for $\delta^{18}O$ and $\Delta^{17}O$, respectively (Savarino et al., 2007), and in the interior of Antarctica (Erbland et al., 2013; Frey et al., 2009). Multifactorial analysis indicated strong correlations of $\delta^{18}O$ with temperature (R^2 = 0.72) and O_3 mixing ratio (R^2 = 0.87; Table S2). These correlations may be linked by the strong $\delta^{18}O(NO_3^-)$ seasonal pattern, in which values were lowest during the late austral spring and austral summer and highest during austral winter and early austral spring. A comparison between $\delta^{18}O$ and $\Delta^{17}O$ indicated a modest positive linear correlation (R^2 = 0.46; Table S2). This modest correlation might indicate that the O isotopic composition of the collected NO_3^- was not a simple mixture between two atmospheric oxidants as previously observed at DDU (Savarino et al., 2007) and Summit, Greenland (Fibiger et al., 2016), but instead may have been influenced by multiple atmospheric oxidants with different $\delta^{18}O$ and $\Delta^{17}O$ values that were incorporated into atmospheric NO_3^- through NO_x oxidation (Michalski et al., 2012; Figure 4).

3.2.2. Sulfate

Measured $\delta^{34}S(SO_4^{2-})_{(TSP)}$ values ranged from 11.9‰ to 21.2‰ (Table 3). We note that multiple filter samples were often combined, particularly during austral winter, to provide enough sample for isotopic analysis (Table 3). The observed $\delta^{34}S(SO_4^{2-})_{(TSP)}$ range was similar to that reported recently for $\delta^{34}S(nss\text{-}SO_4^{2-})$ in the Southern Ocean of 6.0‰ to 19.0‰ (Li et al., 2018). These ranges are bracketed by the $\delta^{34}S$ values of the presumed major SO_4^{2-} sources including DMS emissions = 18.6±1.9‰ (Patris et al., 2002; Sanusi et al., 2006), sea salt SO_4^{2-} = 21±0.1‰ (Rees et al., 1978), continental SO_4^{2-} (3±3‰; Jenkins & Bao, 2006; Li & Barrie, 1993; Norman et al., 1999), and stratospheric SO_4^{2-} = 2.6±0.3‰ (Castleman Jr et al., 1974). $\delta^{34}S(SO_4^{2-})_{(TSP)}$ had a distinct seasonal cycle, with highest values (17.7‰ to 21.2‰) near the beginning of the year between January and April. After reaching a peak value of 21.2‰ at the beginning of April, $\delta^{34}S(SO_4^{2-})_{(TSP)}$ decreased to baseline value between 13‰ and 15‰ that remained relatively constant with an average of 13.9 ± 1.2‰ (n = 8) until our collection period ended (mid-October).

Measured $\Delta^{17}O(SO_4^{2-})_{(TSP)}$ values had a narrow range from 0.8‰ to 1.8‰ (Table 3). Peaks in $\Delta^{17}O(SO_4^{2-})_{(TSP)}$ occurred from March to May and from August to mid-October with average values of 1.4 ± 0.2‰ (n = 4) and 1.6 ± 0.1‰ (n = 3), respectively. Because these values are greater than 1‰, contributions from O_3 aqueous-phase oxidation pathway are expected (Alexander et al., 2005; Table 3). The $\Delta^{17}O(SO_4^{2-})_{(TSP)}$ record was similar to that previously observed at Dome C (Hill-Falkenthal et al., 2013) after adjustments to account for sea salt influence to be consistent with our data (Figure 2). Measured $\delta^{18}O(SO_4^{2-})_{(TSP)}$ values ranged from −12.8‰ to 8.5‰ (Table 3). Generally, $\delta^{18}O(SO_4^{2-})_{(TSP)}$ was lowest during austral summer and highest during austral winter (Figure 2). Values of $\delta^{18}O(SO_4^{2-})_{(TSP)}$ and $\Delta^{17}O(SO_4^{2-})_{(TSP)}$ were weakly correlated (R^2 = 0.11; Table S3), possibly indicating that $\delta^{18}O(SO_4^{2-})_{(TSP)}$ and $\Delta^{17}O(SO_4^{2-})_{(TSP)}$ were influenced by mixing between SO_2 sources and reactions with several different atmospheric oxidants (e.g., O_3, O_2, and H_2O_2), as well as by mixing of primary (e.g., sea salt) and secondary SO_4^{2-}, as previously indicated for South Pole snow pit samples (Shaheen et al., 2013). However, quantitative interpretation of $\delta^{18}O(SO_4^{2-})_{(TSP)}$ was difficult due to isotopic equilibration between SO_2 and H_2O vapor that is quickly achieved (Holt et al., 1981). Therefore, the oxidation dynamics involving $SO_4^{2-}{}_{(TSP)}$ were evaluated utilizing only $\Delta^{17}O(SO_4^{2-})_{(TSP)}$.

4. Discussion

4.1. NO_3^- Seasonal Cycle

4.1.1. $\delta^{15}N(NO_3^-)$

The correlations between solar irradiance and $[NO_3^-]$ (R^2 = 0.59) and $\delta^{15}N(NO_3^-)$ (R^2 = 0.55) indicated that localized snowpack photolysis played a key role in controlling NO_3^-, which has important implications for the oxidative environment at the South Pole (Chen et al., 2004). During periods of sunlight, $[NO_3^-]$ was

21698996, 2019, 14, Downloaded from https://agupubs.onlinelibrary.wiley.com/doi/10.1029/2019JD030517 by Cochrane France, Wiley Online Library on [11/11/2024]. See the Terms and Conditions (https://onlinelibrary.wiley.com/terms-and-conditions) on Wiley Online Library for rules of use; OA articles are governed by the applicable Creative Commons License

Table 3
Summary of Average $[SO_4^{2-}]_{(TSP)}$, Temperature (Temp), Relative Humidity (RH), Solar Radiation, and $[O_3]$ for Each Collection Period Corresponding to $SO_4^{2-}{}_{(TSP)}$ Isotopic Composition Measurement (See Text for Details)

Collection date	Avg [p-SO_4^{2-}] (ng/m^3)	Temp (°C)[a]	RH(%)[a]	Solar irradiance (W/m^2)[a]	$[O_3]$ (ppb$_v$)[a]	$\delta^{34}S(\pm0.3‰)$	$\delta^{18}O(\pm2‰)$	$\Delta^{17}O(\pm0.2‰)$
1/26-2/1 (1)	115.3	−35.2±2.5	71.9±4.3	301.1±36.6	22.6±3.6	18.3	−12.8	0.9
2/1-2/9 (1)	211.4	−37.2 ±0.9	66.7±1.7	273.7±19.1	22±3.4	17.7	−11.3	0.8
2/9-2/16 (1)	124.8	−38.7±2.4	69.4±5.4	209.6±34.9	20.8 ±1.1	18.0	−9.1	1.0
2/16-2/23 (1)	266.3	−39.3±6.2	70.3±5.0	170.1±21.3	20.4±1.0	18.6	−11.6	0.9
2/23-3/1 (1)	172.8	−46.2±3.7	68.4±6.4	106.7±30	20.5±1.2	18.3	−10.4	0.9
3/1-3/8 (1)	107.8	−47.4±4.5	69.8±2.5	82.9±18.7	19.8±1.4	18.9	−12.2	0.9
3/8-3/22 (2)	124.9	−49.3±5.4	69.5±4.3	24.9±15.5	21.4±1.4	18.8	−2.8	1.8
3/22-4/5 (2)	59.9	−52.9±10	65.8±6.7	1.5±1.8	22.6±0.8	21.2	−3.9	1.2
4/5-4/19 (2)	47.5	−50.1±9.0	66.6±4.7	0±0	24.1±1.0	18.2	−5.5	1.3
4/19-5/24 (5)	15.5	−57.9 ±6.0	63.3±4.7	0±0	27.9±2.3	17.4	−0.1	1.2
5/24-6/28 (5)	17.1	−59.4±8.7	64.1±6.0	0±0	32.3±1.1	13.5	2.7	1.0
6/28-7/19 (3)	13.0	−53.7±8.8	67±7.7	0±0	34.1±0.7	15.6	7.0	1.1
7/19-8/2 (2)	16.1	−56.5±8.3	64.9±6.4	0±0	34.4±1.1	13.3	5.0	1.2
8/2-8/23 (3)	12.5	−55.7±10	65.2±6.1	0±0	34.4±1.3	14.3	6.9	0.8
8/23-9/13 (3)	18.5	−57.8±7.4	65.2±5.0	0±0	33.4±1.5	12.7	7.6	1.1
9/13-9/20 (1)	67.1	−54.8±7.6	64.9±3.6	1.2±1.0	32.4±1.0	—	1.5	1.4
9/20-10/4 (1)	27.9	−59.4±5.5	64.5±4.9	19.2±15.8	32.4±1.6	14.7	0.6	1.6
10/4-10/11 (1)	44.8	−48.4±6.4	68.9±3.8	62±23.1	33.4±1.2	—	8.5	1.6
10/11-10/18 (1)	54.9	−55.1±1.8	64.2±2.6	126.6±24.5	30.8±1.2	11.9	−3.2	1.7
10/18-10/25 (1)	70.5	−49.2±3.8	68.5±4.2	148.3±25.5	31.4±0.8	15.4	−3.6	1.5

Note. Parentheses indicate the number of weekly collected filter samples combined for isotopic analysis.
[a]Data obtained from the South Pole Observatory (NOAA; https://www.esrl.noaa.gov/gmd/dv/data/index.php?site=SPO); reported as $\bar{x}\pm1\sigma$ for the specified collection period.

highest (45.0 ± 23.6 ng/m^3, $n = 9$) and $\delta^{15}N(NO_3^-)$ was lowest (−47.0±11.7‰, $n = 5$; Figure 1), consistent with other studies in Antarctica (Erbland et al., 2013; Frey et al., 2009; Ishino et al., 2017; Savarino et al., 2007). Such extremely low values of $\delta^{15}N(NO_3^-)$ typically are not found in midlatitudes but apparently occur only in Antarctica because the chemical and physical processes related to snowpack NO_3^- photolysis have a large N isotope fractionation constant (ε) near −48‰ (Berhanu et al., 2014; Berhanu et al., 2015). This favors the release of NO_x depleted in ^{15}N and can explain the extremely low aerosol $\delta^{15}N(NO_3^-)$ values found during periods of sunlight. The exportation out of the continental ice sheet of this locally produced NO_3^- with extremely low $\delta^{15}N(NO_3^-)$ values may explain the low $\delta^{15}N(NO_3^-)$ values observed in the Antarctic Dry Valleys region (Jackson et al., 2016; Michalski et al., 2005).

During periods of darkness, $\delta^{15}N(NO_3^-)$ increased to an average of 1.0 ± 6.8‰ ($n = 4$), reflecting contributions from another source of NO_3^- with a higher $\delta^{15}N$ end-member. This source is likely derived from long-range transport of continental NO_3^- (Lee et al., 2014; Savarino et al., 2007) and/or stratospheric NO_3^- denitrification (Savarino et al., 2007) during periods of darkness, with estimated $\delta^{15}N(NO_3^-)$ values of 2.5±12.5‰ (Elliott et al., 2009; Freyer, 1978; Heaton, 1987) and 19±3‰ (Savarino et al., 2007), respectively. Previous modeling of NO_3^- over Antarctica has indicated a low background level of $[NO_3^-]$ during May and July, consistent with our observations (Figure 1; Lee et al., 2014). This source of NO_3^- has been modeled to result from NO_x emissions from fossil fuel combustion, soil emissions, and lightning originating from 25° to 65°S that is transported to Antarctica resulting from its formation above continental source regions at an altitude of 5–11 km (Lee et al., 2014). Modeling has also indicated that the slight peak in $[NO_3^-]$ during August (Figure 1) may have resulted from the increasing importance of long-range transported peroxyacetyl nitrate (PAN) and subsequent thermal decomposition and influences from stratospheric denitrification (Lee et al., 2014). Both potential sources are consistent with our measured $\delta^{15}N(NO_3^-)$ at the South Pole during austral winter. We note that while $\delta^{15}N$ values of PAN are uncertain, as the isotopic fractionation associated with PAN formation and decomposition are unknown, these values are likely similar to the continental (or anthropogenic) NO_3^- of 2.5±12.5‰ (Elliott et al., 2009; Freyer, 1978; Heaton, 1987).

21698996, 2019, 14, Downloaded from https://agupubs.onlinelibrary.wiley.com/doi/10.1029/2019JD030517 by Cochrane France, Wiley Online Library on [11/11/2024]. See the Terms and Conditions (https://onlinelibrary.wiley.com/terms-and-conditions) on Wiley Online Library for rules of use; OA articles are governed by the applicable Creative Commons License

21698996, 2019, 14, Downloaded from https://agupubs.onlinelibrary.wiley.com/doi/10.1029/2019JD030517 by Cochrane France, Wiley Online Library on [11/11/2024]. See the Terms and Conditions (https://onlinelibrary.wiley.com/terms-and-conditions) on Wiley Online Library for rules of use; OA articles are governed by the applicable Creative Commons License

4.1.2. Nitrate $\Delta^{17}O$ and $\delta^{18}O$

The measured seasonal record of $\Delta^{17}O(NO_3^-)$ matched closely with that previously reported for NO_3^- aerosols collected at the South Pole in 2003 to 2004 (McCabe et al., 2007), which was attributed to localized tropospheric oxidation chemistry during austral summer and a combination of stratospheric denitrification and transported nitrate from the lower latitudes during austral winter. Tropospheric oxidation can result in $\Delta^{17}O(NO_3^-)$ values that range from 17.3‰ to 42.3‰, which reflects NO_x cycling with O_3, RO_2 (or HO_2), and reactive halogens (XO; most notably BrO) and subsequent NO_2 oxidation that may incorporate O atoms derived from O_3, H_2O, and/or OH in the product NO_3^- (Michalski et al., 2003; Morin et al., 2009; Table 1). Elevated $\Delta^{17}O(NO_3^-)$ values of stratospheric NO_3^- are suspected to exist due to elevated stratospheric $\Delta^{17}O(O_3)$ values (Janssen, 2005) in comparison to tropospheric O_3 and/or elevated $ClONO_2$ $\Delta^{17}O$ values (McCabe et al., 2007) when $ClONO_2$ is the dominant source of stratospheric NO_3^- during the polar vortex ((R1) and (R2)):

$$ClO + NO_2 \longrightarrow ClONO_2, \tag{R1}$$

$$ClONO_2 + HCl \longrightarrow HNO_3 + Cl_2. \tag{R2}$$

This framework is consistent with the measured $\Delta^{17}O(NO_3^-)$ values that were within the general expected troposphere $\Delta^{17}O(NO_3^-)$ range during austral summer, fall, and spring (21.8‰ to 32.4‰), reflecting tropospheric NO_3^- formation contributions by NO_2 + OH oxidation that tended to be higher during periods of sunlight due to elevated OH concentrations. The high $\Delta^{17}O(NO_3^-)$ observed during austral winter (41.1‰) likely reflected tropospheric nitrate formation dominated by NO_3 + RH or halogen hydrolysis during the absence of sunlight and/or stratospheric denitrification.

To further constrain NO_3^- oxidation pathways, we considered $\delta^{18}O$-$\Delta^{17}O$ relations for major tropospheric O bearing molecules incorporated into NO_3^- (Figure 4; Fibiger et al., 2016; Michalski et al., 2012). Here we assume that the O isotopic composition of NO_3^- is derived from a mixture between a high $\delta^{18}O$-$\Delta^{17}O$ end-member, $O_{3(terminal)}$ and XO ($\delta^{18}O$ = 95–115‰; Johnston & Thiemens, 1997), $\Delta^{17}O$ =39.3±2.0‰ (Vicars & Savarino, 2014), and various low $\delta^{18}O$-$\Delta^{17}O$ end-members including $O_2/RO_2/HO_2$ ($\delta^{18}O$ = 23.5‰, $\Delta^{17}O$ = 0‰; Kroopnick & Craig, 1972), H_2O ($\delta^{18}O$ = −27.5±20‰, $\Delta^{17}O$ = 0‰) and OH ($\delta^{18}O$ = -70±20‰, $\Delta^{17}O$ = 0‰) (Michalski et al., 2012). We note that OH may not attain complete isotopic equilibrium with H_2O vapor in polar regions because of low water mixing ratios (Morin et al., 2007). If OH maintains some of its O_3 character from $O(^1D)$, the mixing line between O_3 and OH remains the same, with the O atom incorporated into NO_3^- shifted toward O_3 (Fibiger et al., 2016). We note that due to the speculative nature of $\delta^{18}O$ values of some of the major O bearing molecules, it can be difficult to use this to evaluate oxidation pathways quantitatively, but it may provide some additional qualitative constraints.

From $\delta^{18}O$-$\Delta^{17}O$ relations, austral summer NO_3^- tended to mix between $O_{3(term)}$ and OH, indicating that NO_3^- was primarily formed through the NO_2 + OH + M→ HNO_3 + M oxidation pathway. Elevated [OH] has been measured during the austral summer at the South Pole (as high as 2.0×10^6 molecules/cm^3; Mauldin et al., 2001). If OH oxidation dominated austral summer NO_3^- formation, then based on $\Delta^{17}O$ mass balance, the starting NO_2 would have had a $\Delta^{17}O$ of 41.4‰, indicating near complete NO_x cycling with O_3. This is unrealistic due to the high HO_x concentration in austral summer in the interior of Antarctica (Savarino et al., 2016), indicating that unknown processes appeared to play a substantial role in the atmospheric NO_3^- budget during austral summer at the South Pole, which has also been reported for Dome C (Savarino et al., 2016). Austral fall NO_3^- tended to shift toward a mixture involving $O_{3(term)}$ and O_2, which indicates incorporation of O atoms derived from RO_2/HO_2 during NO_x photochemical cycling. This is consistent with model results for the middle to high latitude of the Southern Hemisphere that predicted the dominant post-NO_2 oxidation pathways include both NO_2 + OH (daytime dominant) and NO_3 + DMS (nighttime dominant) pathways (Alexander et al., 2009). Because the South Pole was dark during this period, (i.e., absence of NO_x photochemical cycling), this indicates that some of the NO_3^- during austral fall was derived from long-range transport, consistent with the $\delta^{15}N(NO_3^-)$ values measured during this collection period, conclusions drawn for NO_3^- collected during the austral fall at DDU (Savarino et al., 2007), and

21698996, 2019, 14, Downloaded from https://agupubs.onlinelibrary.wiley.com/doi/10.1029/2019JD030517 by Cochrane France, Wiley Online Library on [11/11/2024]. See the Terms and Conditions (https://onlinelibrary.wiley.com/terms-and-conditions) on Wiley Online Library for rules of use; OA articles are governed by the applicable Creative Commons License

model expectations (Lee et al., 2014). Austral winter $\delta^{18}O$-$\Delta^{17}O$ indicated that all O atoms are derived from $O_{3(term)}$, indicating that either high end-member $\delta^{18}O$-$\Delta^{17}O$ tropospheric oxidation pathways (e.g., NO_3 + DMS or $XONO_2$ hydrolysis) played an important role in NO_3^- formation or stratospheric denitrification was important. Finally, austral spring NO_3^- tracked between $O_{3(term)}$ and RO_2 (or HO_2) and OH. We note that austral springtime mixing relations overlap with $O_{3(term)}$ and H_2O mixing, but the N_2O_5 hydrolysis pathway was expected to play a minor role over the South Pole during this period (Alexander et al., 2009). Because of snowpack photolysis returns during this period of constant sunlight, local oxidation was expected to dominate the NO_3^- formed at the South Pole as supported by our $\delta^{15}N(NO_3^-)$ results. This indicates that RO_2 (and/or HO_2) chemistry played an important role in NO_x photochemical cycling leading to elevated localized $[O_3]$ (Crawford et al., 2001). Post-NO_2 oxidation was likely a combination of daytime pathways including NO_2 + OH and $XONO_2$ hydrolysis (Alexander et al., 2009). These two pathways have opposite $\delta^{18}O$-$\Delta^{17}O$ mixing end-members (e.g., Figure 4) and likely account for the observed midranged NO_3^- $\delta^{18}O$-$\Delta^{17}O$ values during austral spring.

4.2. SO_4^{2-} Seasonal Cycle

4.2.1. $\delta^{34}S(SO_4^{2-})_{(TSP)}$

Elevated $[SO_4^{2-}]_{(TSP)}$ (86.7 ± 73.7 ng/m^3, n = 17) occurred during austral summer and fall when biogenic activity (e.g., DMS emissions) was highest (January–May), which is supported by an average $\delta^{34}S(SO_4^{2-})_{(TSP)}$ of 18.5±1.0‰ (n = 10) that was indistinguishable from the DMS $\delta^{34}S$ value of 18.6±1.9‰ (Patris et al., 2002; Sanusi et al., 2006). This indicates that the combined influence of DMS oxidation to SO_4^{2-} and transport to the South Pole during the austral summer and early fall resulted in minimal $\delta^{34}S$ isotopic fractionation. During austral winter (June–August), $[SO_4^{2-}]_{(TSP)}$ decreased to a baseline level of approximately 15.3 ng/m^3 that was accompanied by a decrease in the average $\delta^{34}S(SO_4^{2-})_{(TSP)}$ to 14.2 ± 0.9‰ (n = 4). The $[SO_4^{2-}]_{(TSP)}$ decrease was a result of substantially less biogenic sulfur production during this period in the Southern Hemisphere, which is supported by the accompanying decrease in wintertime $\delta^{34}S(SO_4^{2-})_{(TSP)}$. This indicated a potentially larger SO_4^{2-} contribution from a nonbiogenic source with a low $\delta^{34}S(SO_4^{2-})$ end-member value such as transported continental SO_4^{2-} (including volcanic, mineral, continental biogenic, and anthropogenic sources; Patris et al., 2000; $\delta^{34}S$ = 3±3‰; Jenkins & Bao, 2006; Li & Barrie, 1993; Norman et al., 1999), stratospheric intrusions ($\delta^{34}S$ = 2.6±0.3‰; Castleman Jr et al., 1974), and localized passive volcanic emission of SO_2 ($\delta^{34}S$ = 0 to 5‰; Liotta et al., 2012). At the end of austral winter and early spring (September–October), $[SO_4^{2-}]_{(TSP)}$ increased to 29.6 ± 19.0 ng/m^3 (n = 7), and the mass-weighted $\delta^{34}S(SO_4^{2-})_{(TSP)}$ was 13.7 ± 1.4‰ (n = 4), which was lower than that observed during austral winter. Previous studies in the Southern Ocean have indicated that austral spring-time $SO_4^{2-}{}_{(NSS)}$ tended to be dominated by DMS emissions (Li et al., 2018). Thus, the increase in $SO_4^{2-}{}_{(TSP)}$ during this period likely reflected the increased emission of DMS, but relatively low $\delta^{34}S(SO_4^{2-})_{(TSP)}$ during this period again highlights the potential importance of a nonbiogenic $SO_4^{2-}{}_{(TSP)}$ source with a low-end-member $\delta^{34}S(SO_4^{2-})$ value.

We note that the relative SO_4^{2-} contribution from sea salt was highest in the interior of Antarctica during austral winter and spring, with relative contributions of ~33% and ~20% reported for May to August and September to October compared to only ~8% for November to April, at Dome C (Hill-Falkenthal et al., 2013). A potentially higher contribution from sea salt SO_4^{2-} cannot explain the lower $\delta^{34}S(SO_4^{2-})$ values observed during austral winter and spring based on mass balance alone because it has a high end-member $\delta^{34}S$ value of 21±0.1‰ (Rees et al., 1978), indicating the potential increased importance of a nonbiogenic nss-SO_4^{2-} source with a low $\delta^{34}S$ value. However, previous work in the interior of Antarctica (Concordia) has shown that biogenic-derived SO_4^{2-} dominated the nss-SO_4^{2-} budget year-round with a contribution from a nonbiogenic nss-SO_4^{2-} source of no more than 1 ng/m^3 during austral fall and austral winter and 5 ng/m^3 during austral spring (Legrand et al., 2017). If these contributions are similar at the South Pole, it would have represented approximately 6.5% and 16.9% of $[SO_4^{2-}]_{(TSP)}$ during austral winter and spring, respectively. Assuming an average $\delta^{34}S$ of 19.9‰ for the marine-derived SO_4^{2-} sources (e.g., DMS and sea salt) and 0‰ for nonmarine (or nonbiological nss-SO_4^{2-}) sources (e.g., anthropogenic, stratosphere, and volcano) and applying $\delta^{34}S(SO_4^{2-})$ mass balance (equation (3)), this would indicate an expected $\delta^{34}S(SO_4^{2-})_{(TSP)}$ value of 18.6‰ and 16.5‰ during austral winter and spring, respectively.

$$\delta^{34}S\left(SO_4^{2-}\right)_{TSP} = f_{\text{Marine}}\left[\delta^{34}S\left[SO_4^{2-}\right]\right]_{\text{Marine}} + f_{\text{Nonmarine}}\left[\delta^{34}S\left[SO_4^{2-}\right]\right]_{\text{Nonmarine}} \quad (3)$$

where $\delta^{34}S(SO_4^{2-})_{(TSP)}$ was the measured value and f_{Marine} and $f_{\text{Nonmarine}}$ refer to the fraction of $SO_4^{2-}{}_{(TSP)}$ derived from marine (e.g., DMS and sea salt) and nonmarine (e.g., nonbiological nss-SO_4^{2-} including anthropogenic, stratospheric, and/or volcanoes) sources, respectively. These estimated values are higher than the observed values of 14.2 ± 0.9‰ ($n = 4$) and 13.7 ± 1.4‰ ($n = 4$) during these periods, respectively. This indicates that either the contribution of nonmarine (or nonbiogenic nss-SO_4^{2-}) was higher at the South Pole or there was a substantial $\delta^{34}S$ isotope effect during oxidation and/or transport to the South Pole during these periods. Back-calculating the $f_{\text{Nonmarine}}$ (equation (3)) would indicate a relative contribution of a nonbiological nss-SO_4^{2-} source of 28.6% and 31.1% to match the measured $\delta^{34}S(SO_4^{2-})_{(TSP)}$, representing approximately 4.4 and 9.2 ng/m^3 during austral winter and spring, respectively. While these values are much larger than reported for Concordia (Legrand et al., 2017), they are within estimated upper limits for the interior of Antarctica of 6 ng/m^3 during austral winter and 11 ng/m^3 during austral summer (Hill-Falkenthal et al., 2013; we note that the expected upper limit for austral fall was not estimated but should be between 6 and 11 ng/m^3). This result highlights potential differences in the SO_4^{2-} budget in the interior of Antarctica; however, we note that this calculation implies no $\delta^{34}S$ fractionation during oxidation to SO_4^{2-} and/or transport to the South Pole. Additional work is warranted to further diagnose the seasonal contributions to SO_4^{2-} budget at the South Pole. Nonetheless, while there may have been some uncertainties in the relative contribution of nonbiogenic nss-SO_4^{2-} to the South Pole, the year-round elevated $\delta^{34}S(SO_4^{2-})$ indicated the dominant role of DMS emissions and its subsequent oxidation and transport to the overall SO_4^{2-} budget at the South Pole. This finding is consistent with previous studies in the interior of Antarctica (Legrand et al., 2017).

4.2.2. $\Delta^{17}O(SO_4^{2-})_{(TSP)}$

The measured $\Delta^{17}O(SO_4^{2-})_{(TSP)}$ values at the South Pole had a somewhat similar seasonal cycle as reported at Dome C (Figure 2). Typically, lowest values were observed during austral summer ($\Delta^{17}O = 0.9 \pm 0.1$‰; $n = 5$) and during austral winter (1.0±0.2‰; $n = 4$) reflecting greater contributions from OH, H_2O_2, and HOBr (or HOCl) oxidation pathways (Figure 2). Highest $\Delta^{17}O$ values occurred during austral fall (1.3 ± 0.3‰, $n = 6$) and austral spring (1.6±0.1‰, $n = 5$). These $\Delta^{17}O$ values are greater than 1‰, indicating contributions from aqueous O_3 oxidation. The maximum contribution from S (IV) + O_3 oxidation for each SO_4^{2-} sample was calculated assuming no contribution from H_2O_2 (equation (4); Chen et al., 2016):

$$f_{O_{3,\max}} = \frac{\Delta^{17}O_{obs}\left(SO_4^{2-}\right)}{\Delta^{17}O\left(SO_4^{2-}\right)_{O_3}}, \quad (4)$$

where $\Delta^{17}O(SO_4^{2-})_{O3} = 9.9$‰. In a similar manner, the minimum contribution from O_3 oxidation was estimated assuming that H_2O_2 is the only other oxidation pathway (equation (5); Chen et al., 2016):

$$f_{O_{3,\min}} = \frac{\Delta^{17}O_{obs}\left(SO_4^{2-}\right) - \Delta^{17}O\left(SO_4^{2-}\right)_{H_2O_2}}{\Delta^{17}O\left(SO_4^{2-}\right)_{O_3} - \Delta^{17}O\left(SO_4^{2-}\right)_{H_2O_2}}, \quad (5)$$

where $\Delta^{17}O(SO_4^{2-})_{H2O2} = 0.8$‰ (Table 1). This yielded an estimated O_3 contribution range (minimum to maximum) of 0.02–0.09, 0.06–0.13, 0.04–0.11, and 0.10–0.16 for austral summer, fall, winter, and spring, respectively. Thus, O_3 oxidation appeared to have played the largest role during austral spring and smallest role during austral summer. A relatively minor contribution from O_3 oxidation during austral summer was not surprising given the strong role of HO_x chemistry and HOX during this period. We note that our estimate of f_{O3} for wintertime $SO_4^{2-}{}_{(TSP)}$ might be influenced by a possible higher contribution during this period from ss-SO_4^{2-} with a $\Delta^{17}O = 0$‰, which we cannot accurately evaluate with our data set. Assuming a similar ss-SO_4^{2-} contribution in our samples as found at Dome C in austral winter of ~0.33, our estimated f_{O3} range increased to 0.09–0.16.

5. Conclusions

Aerosol samples were collected over a 10-month period at the South Pole in 2002, and a combination of concentration and isotopic analysis was used to evaluate the dynamics of NO_3^- and $SO_4^{2-}{}_{(TSP)}$. NO_3^- variations

21698996, 2019, 14, Downloaded from https://agupubs.onlinelibrary.wiley.com/doi/10.1029/2019JD030517 by Cochrane France, Wiley Online Library on [11/11/2024]. See the Terms and Conditions (https://onlinelibrary.wiley.com/terms-and-conditions) on Wiley Online Library for rules of use; OA articles are governed by the applicable Creative Commons License

21698996, 2019, 14, Downloaded from https://agupubs.onlinelibrary.wiley.com/doi/10.1029/2019JD030517 by Cochrane France, Wiley Online Library on [11/11/2024]. See the Terms and Conditions (https://onlinelibrary.wiley.com/terms-and-conditions) on Wiley Online Library for rules of use; OA articles are governed by the applicable Creative Commons License

were found to be driven by seasonal snowpack photolysis that resulted in elevated $[NO_3^-]$ with low $\delta^{15}N(NO_3^-)$ values (−47.0±11.7‰, $n = 5$) because of localized atmospheric recycling during periods of sunlight at the South Pole. The seasonal cycle of $\Delta^{17}O(NO_3^-)$ at the South Pole indicated tropospheric chemistry dominated NO_3^- formation year-round with possible stratospheric denitrification contributions during austral winter. Seasonal $[SO_4^{2-}]_{(TSP)}$ had some similarities with $[NO_3^-]$, with the highest values observed during austral summer and lowest values during austral winter. Summertime elevated $[SO_4^{2-}]_{(TSP)}$ appeared to be derived from transported biogenic sulfur emissions as indicated by $\delta^{34}S(SO_4^{2-})_{(TSP)}$ of 18.5±1.0‰ ($n = 10$) that is similar to the marine biogenic $\delta^{34}S$ value. Values of $\Delta^{17}O(SO_4^{2-})_{(TSP)}$ were approximately uniform year-round (0.8‰ to 1.8‰), with highest values observed during austral fall and spring. The seasonal variation in $\Delta^{17}O(SO_4^{2-})_{(TSP)}$ is influenced by changes in oxidation chemistry as well as potentially larger relative contributions from ss-SO_4^{2-} during austral winter.

The observed seasonal cycles in the isotopic compositions of NO_3^- and SO_4^{2-} were similar to those previously observed in the interior of Antarctica including South Pole, Dome C, on the East Antarctic, and at the coast at DDU. This is an important finding and indicates that the atmosphere and the snowpack chemistry involving NO_3^- and SO_4^{2-} tend to behave uniformly across the plateau and that a regional signal can be expected from ice core measurements in Antarctica. Characterization of regional processes will enable further understanding of NO_3^- and SO_4^{2-} connections with climate feedback processes on both short and long time scales, as direct anthropogenic inputs derived from continental long-range transport tended to play a minor role on the overall NO_3^- and SO_4^{2-} budgets in the interior of Antarctica. While these are potentially important findings, we note that isotope data for both NO_3^- and SO_4^{2-} are still relatively limited in Antarctica. Further analysis is needed, including multiple yearlong investigations of NO_3^- and SO_4^{2-} in aerosol samples across several sites. Recent methodological developments have substantially reduced the sample requirements for isotopic analysis, particularly for NO_3^-, which will increase our ability to further diagnose its temporal variabilities in the Antarctic plateau.

Acknowledgments

W. W. W. acknowledges support from an Atmospheric and Geospace Sciences National Science Foundation Postdoctoral Fellow (Grant 1624618). We acknowledge support from the Purdue Climate Change Research Center. The authors declare no financial conflicts of interest. We thank the South Pole Observatory and the National Oceanic and Atmospheric Administration Earth System Research Laboratory Global Monitoring Division for access to ancillary meteorology and ozone data. The authors thank three anonymous reviewers and Lucy Rose for their helpful suggestions that significantly improved the manuscript. Any use of trade, firm, or product names in this paper is for descriptive purposes only and does not imply endorsement by the U.S. Government. Data presented in this manuscript are available within the text (Tables 2 and 3).

References

Adams, P. J., Seinfeld, J. H., & Koch, D. M. (1999). Global concentrations of tropospheric sulfate, nitrate, and ammonium aerosol simulated in a general circulation model. *Journal of Geophysical Research*, *104*(D11), 13,791–13,823. https://doi.org/10.1029/1999JD900083

Alexander, B., Hastings, M. G., Allman, D. J., Dachs, J., Thornton, J. A., & Kunasek, S. A. (2009). Quantifying atmospheric nitrate formation pathways based on a global model of the oxygen isotopic composition ($\Delta^{17}O$) of atmospheric nitrate. *Atmospheric Chemistry and Physics*, *9*(14), 5043–5056. https://doi.org/10.5194/acp-9-5043-2009

Alexander, B., Park, R. J., Jacob, D. J., Li, Q. B., Yantosca, R. M., Savarino, J., et al. (2005). Sulfate formation in sea-salt aerosols: Constraints from oxygen isotopes. *Journal of Geophysical Research*, *110*, D10307. https://doi.org/10.1029/2004JD005659

Alexander, B., Savarino, J., Kreutz, K. J., & Thiemens, M. H. (2004). Impact of preindustrial biomass-burning emissions on the oxidation pathways of tropospheric sulfur and nitrogen. *Journal of Geophysical Research*, *109*, D08303. https://doi.org/10.1029/2003JD004218

Alexander, B., Thiemens, M. H., Farquhar, J., Kaufman, A. J., Savarino, J., & Delmas, R. J. (2003). East Antarctic ice core sulfur isotope measurements over a complete glacial-interglacial cycle. *Journal of Geophysical Research*, *108*(D24), 4786. https://doi.org/10.1029/2003JD003513

Arimoto, R., Nottingham, A. S., Webb, J., Schloesslin, C. A., & Davis, D. D. (2001). Non-sea salt sulfate and other aerosol constituents at the South Pole during ISCAT. *Geophysical Research Letters*, *28*(19), 3645–3648. https://doi.org/10.1029/2000GL012714

Augustin, L., Barbante, C., Barnes, P. R., Barnola, J. M., Bigler, M., Castellano, E., et al., & EPICA community members (2004). Eight glacial cycles from an Antarctic ice core. *Nature*, *429*(6992), 623–628. https://doi.org/10.1038/nature02599

Barkan, E., & Luz, B. (2003). High-precision measurements of $^{17}O/^{16}O$ and $^{18}O/^{16}O$ of O_2 and O_2/Ar ratio in air. *Rapid Communications in Mass Spectrometry*, *17*(24), 2809–2814. https://doi.org/10.1002/rcm.1267

Barkan, E., & Luz, B. (2005). High precision measurements of $^{17}O/^{16}O$ and $^{18}O/^{16}O$ ratios in H_2O. *Rapid Communications in Mass Spectrometry*, *19*(24), 3737–3742. https://doi.org/10.1002/rcm.2250

Barnola, J.-M., Raynaud, D., Korotkevich, Y. S., & Lorius, C. (1987). Vostok ice core provides 160,000-year record of atmospheric CO_2. *Nature*, *329*(6138), 408–414. https://doi.org/10.1038/329408a0

Berhanu, T. A., Meusinger, C., Erbland, J., Jost, R., Bhattacharya, S. K., Johnson, M. S., & Savarino, J. (2014). Laboratory study of nitrate photolysis in Antarctic snow. II. Isotopic effects and wavelength dependence. *The Journal of Chemical Physics*, *140*(24), 244306. https://doi.org/10.1063/1.4882899

Berhanu, T. A., Savarino, J., Erbland, J., Vicars, W. C., Preunkert, S., Martins, J. F., & Johnson, M. S. (2015). Isotopic effects of nitrate photochemistry in snow: A field study at Dome C, Antarctica. *Atmospheric Chemistry and Physics*, *15*(19), 11,243–11,256. https://doi.org/10.5194/acp-15-11243-2015

Böhlke, J. K., Gwinn, C. J., & Coplen, T. B. (1993). New reference materials for nitrogen-isotope-ratio measurements. *Geostandards Newsletter*, *17*(1), 159–164. https://doi.org/10.1111/j.1751-908X.1993.tb00131.x

Castleman Jr, A. W., Munkelwitz, H. R., & Manowitz, B. (1974). Isotopic studies of the sulfur component of the stratospheric aerosol layer. *Tellus*, *26*(1–2), 222–234.

Chen, G., Davis, D., Crawford, J., Hutterli, L. M., Huey, L. G., Slusher, D., et al. (2004). A reassessment of HO_x South Pole chemistry based on observations recorded during ISCAT 2000. *Atmospheric Environment*, *38*(32), 5451–5461. https://doi.org/10.1016/j.atmosenv.2003.07.018

Chen, Q., Geng, L., Schmidt, J. A., Xie, Z., Kang, H., Dachs, J., et al. (2016). Isotopic constraints on the role of hypohalous acids in sulfate aerosol formation in the remote marine boundary layer. *Atmospheric Chemistry and Physics*, *16*(17), 11,433–11,450. https://doi.org/10.5194/acp-16-11433-2016

Craig, H., Chou, C. C., Welhan, J. A., Stevens, C. M., & Engelkemeir, A. (1988). The isotopic composition of methane in polar ice cores. *Science*, *242*(4885), 1535–1539. https://doi.org/10.1126/science.242.4885.1535

Crawford, J. H., Davis, D. D., Chen, G., Buhr, M., Oltmans, S., Weller, R., et al. (2001). Evidence for photochemical production of ozone at the South Pole surface. *Geophysical Research Letters*, *28*(19), 3641–3644. https://doi.org/10.1029/2001GL013055

Davis, D., Chen, G., Buhr, M., Crawford, J., Lenschow, D., Lefer, B., et al. (2004). South Pole NO_x Chemistry: An assessment of factors controlling variability and absolute levels. *Atmospheric Environment*, *38*(32), 5375–5388. https://doi.org/10.1016/j.atmosenv.2004.04.039

Davis, D., Seelig, J., Huey, G., Crawford, J., Chen, G., Wang, Y., et al. (2008). A reassessment of Antarctic plateau reactive nitrogen based on ANTCI 2003 airborne and ground based measurements. *Atmospheric Environment*, *42*(12), 2831–2848. https://doi.org/10.1016/j.atmosenv.2007.07.039

Delmas, R. J. (2013). *Ice core studies of global biogeochemical cycles*, (Vol. 30). Berlin Heidelberg: Springer Science & Business Media.

Dominguez, G., Jackson, T., Brothers, L., Barnett, B., Nguyen, B., & Thiemens, M. H. (2008). Discovery and measurement of an isotopically distinct source of sulfate in Earth's atmosphere. *Proceedings of the National Academy of Sciences*, *105*(35), 12,769–12,773. https://doi.org/10.1073/pnas.0805255105

Elliott, E. M., Kendall, C., Boyer, E. W., Burns, D. A., Lear, G. G., Golden, H. E., et al. (2009). Dual nitrate isotopes in dry deposition: Utility for partitioning NO_x source contributions to landscape nitrogen deposition. *Journal of Geophysical Research*, *114*, G04020. https://doi.org/10.1029/2008JG000889

Erbland, J., Vicars, W. C., Savarino, J., Morin, S., Frey, M. M., Frosini, D., et al. (2013). Air–snow transfer of nitrate on the East Antarctic Plateau—Part 1: Isotopic evidence for a photolytically driven dynamic equilibrium in summer. *Atmospheric Chemistry and Physics*, *13*(13), 6403–6419. https://doi.org/10.5194/acp-13-6403-2013

Fibiger, D. L., Dibb Jack, E., Dexian, C., Thomas Jennie, L., Burkhart John, F., Gregory, H. L., & Hastings Meredith, G. (2016). Analysis of nitrate in the snow and atmosphere at Summit, Greenland: Chemistry and transport. *Journal of Geophysical Research: Atmospheres*, *121*, 5010–5030. https://doi.org/10.1002/2015JD024187

Fogelman, K. D., Walker, D. M., & Margerum, D. W. (1989). Nonmetal redox kinetics: Hypochlorite and hypochlorous acid reactions with sulfite. *Inorganic Chemistry*, *28*(6), 986–993. https://doi.org/10.1021/ic00305a002

Frey, M. M., Savarino, J., Morin, S., Erbland, J., & Martins, J. M. F. (2009). Photolysis imprint in the nitrate stable isotope signal in snow and atmosphere of East Antarctica and implications for reactive nitrogen cycling. *Atmospheric Chemistry and Physics*, *9*(22), 8681–8696. https://doi.org/10.5194/acp-9-8681-2009

Freyer, H. D. (1978). Seasonal trends of NH_4^+ and NO_3^- nitrogen isotope composition in rain collected at Jülich, Germany. *Tellus*, *30*(1), 83–92.

Friedli, H., Lötscher, H., Oeschger, H., Siegenthaler, U., & Stauffer, B. (1986). Ice core record of the $^{13}C/^{12}C$ ratio of atmospheric CO_2 in the past two centuries. *Nature*, *324*(6094), 237–238. https://doi.org/10.1038/324237a0

Hastings, M. G., Jarvis, J. C., & Steig, E. J. (2009). Anthropogenic impacts on nitrogen isotopes of ice-core nitrate. *Science*, *324*(5932), 1288–1288. https://doi.org/10.1126/science.1170510

Hauglustaine, D. A., Balkanski, Y., & Schulz, M. (2014). A global model simulation of present and future nitrate aerosols and their direct radiative forcing of climate. *Atmospheric Chemistry & Physics*, *14*(20), 11,031–11,063. https://doi.org/10.5194/acp-14-11031-2014

Haywood, J., & Boucher, O. (2000). Estimates of the direct and indirect radiative forcing due to tropospheric aerosols: A review. *Reviews of Geophysics*, *38*(4), 513–543. https://doi.org/10.1029/1999RG000078

Heaton, T. H. E. (1987). $^{15}N^{14}N$ ratios of nitrate and ammonium in rain at Pretoria, South Africa. *Atmospheric Environment (1967)*, *21*(4), 843–852. https://doi.org/10.1016/0004-6981(87)90080-1

Heaton, T. H. E. (1990). $^{15}N/^{14}N$ ratios of NO_x from vehicle engines and coal-fired power stations. *Tellus B*, *42*(3), 304–307.

Helmig, D., Oltmans, S. J., Carlson, D., Lamarque, J. F., Jones, A., Labuschagne, C., et al. (2007). A review of surface ozone in the polar regions. *Atmospheric Environment*, *41*(24), 5138–5161. https://doi.org/10.1016/j.atmosenv.2006.09.053

Hill-Falkenthal, J., Priyadarshi, A., Savarino, J., & Thiemens, M. (2013). Seasonal variations in ^{35}S and $\Delta^{17}O$ of sulfate aerosols on the Antarctic plateau. *Journal of Geophysical Research: Atmospheres*, *118*, 9444–9455. https://doi.org/10.1002/jgrd.50716

Holt, B. D., Kumar, R., & Cunningham, P. T. (1981). Oxygen-18 study of the aqueous-phase oxidation of sulfur dioxide. *Atmospheric Environment (1967)*, *15*(4), 557–566. https://doi.org/10.1016/0004-6981(81)90186-4

Ishino, S., Hattori, S., Savarino, J., Jourdain, B., Preunkert, S., Legrand, M., et al. (2017). Seasonal variations of triple oxygen isotopic compositions of atmospheric sulfate, nitrate, and ozone at Dumont d'Urville, coastal Antarctica. *Atmospheric Chemistry and Physics*, *17*(5), 3713–3727. https://doi.org/10.5194/acp-17-3713-2017

Jackson, A., Davila, A. F., Böhlke, J. K., Sturchio, N. C., Sevanthi, R., Estrada, N., et al. (2016). Deposition, accumulation, and alteration of Cl^-, NO_3^-, ClO_4^- and ClO_3^- salts in a hyper-arid polar environment: Mass balance and isotopic constraints. *Geochimica et Cosmochimica Acta*, *182*, 197–215. https://doi.org/10.1016/j.gca.2016.03.012

Janssen, C. (2005). Intramolecular isotope distribution in heavy ozone ($^{16}O^{18}O^{16}O$ and $^{16}O^{16}O^{18}O$). *Journal of Geophysical Research*, *110*, D08308. https://doi.org/10.1029/2004JD005479

Jenkins, K. A., & Bao, H. (2006). Multiple oxygen and sulfur isotope compositions of atmospheric sulfate in Baton Rouge, LA, USA. *Atmospheric Environment*, *40*(24), 4528–4537. https://doi.org/10.1016/j.atmosenv.2006.04.010

Johnston, J. C., & Thiemens, M. H. (1997). The isotopic composition of tropospheric ozone in three environments. *Journal of Geophysical Research*, *102*(D21), 25,395–25,404. https://doi.org/10.1029/97JD02075

Kaiser, J., Röckmann, T., & Brenninkmeijer, C. A. (2004). Contribution of mass-dependent fractionation to the oxygen isotope anomaly of atmospheric nitrous oxide. *Journal of Geophysical Research*, *109*, D033055. https://doi.org/10.1029/2003JD004088

Kiehl, J. T., Schneider, T. L., Rasch, P. J., Barth, M. C., & Wong, J. (2000). Radiative forcing due to sulfate aerosols from simulations with the National Center for Atmospheric Research Community Climate Model, Version 3. *Journal of Geophysical Research*, *105*(D1), 1441–1457. https://doi.org/10.1029/1999JD900495

Krankowsky, D., Bartecki, F., Klees, G. G., Mauersberger, K., Schellenbach, K., & Stehr, J. (1995). Measurement of heavy isotope enrichment in tropospheric ozone. *Geophysical Research Letters*, *22*(13), 1713–1716. https://doi.org/10.1029/95GL01436

Kroopnick, P., & Craig, H. (1972). Atmospheric oxygen: Isotopic composition and solubility fractionation. *Science*, *175*(4017), 54–55. https://doi.org/10.1126/science.175.4017.54

Lee, C. C.-W., & Thiemens, M. H. (2001). The $\delta^{17}O$ and $\delta^{18}O$ measurements of atmospheric sulfate from a coastal and high alpine region: A mass-independent isotopic anomaly. *Journal of Geophysical Research*, *106*(D15), 17,359–17,373. https://doi.org/10.1029/2000JD900805

21698996, 2019, 14, Downloaded from https://agupubs.onlinelibrary.wiley.com/doi/10.1029/2019JD030517 by Cochrane France, Wiley Online Library on [11/11/2024]. See the Terms and Conditions (https://onlinelibrary.wiley.com/terms-and-conditions) on Wiley Online Library for rules of use; OA articles are governed by the applicable Creative Commons License

Lee, H.-M., Henze, D. K., Alexander, B., & Murray, L. T. (2014). Investigating the sensitivity of surface-level nitrate seasonality in Antarctica to primary sources using a global model. *Atmospheric Environment*, *89*, 757–767. https://doi.org/10.1016/j.atmosenv.2014.03.003

Legrand, M., Preunkert, S., Jourdain, B., Gallée, H., Goutail, F., Weller, R., & Savarino, J. (2009). Year-round record of surface ozone at coastal (Dumont d'Urville) and inland (Concordia) sites in East Antarctica. *Journal of Geophysical Research*, *114*, D20306. https://doi.org/10.1029/2008JD011667

Legrand, M., Preunkert, S., Weller, R., Zipf, L., Elsässer, C., Merchel, S., et al. (2017). Year-round record of bulk and size-segregated aerosol composition in central Antarctica (Concordia site) Part 2: Biogenic sulfur (sulfate and methanesulfonate) aerosol. *Atmospheric Chemistry and Physics*, *17*(22), 14,055–14,073. https://doi.org/10.5194/acp-17-14055-2017

Legrand, M. R., Lorius, C., Barkov, N. I., & Petrov, V. N. (1988). Vostok (Antarctica) ice core: Atmospheric chemistry changes over the last climatic cycle (160,000 years). *Atmospheric Environment (1967)*, *22*(2), 317–331. https://doi.org/10.1016/0004-6981(88)90037-6

Leuenberger, M., Siegenthaler, U., & Langway, C. (1992). Carbon isotope composition of atmospheric CO2 during the last ice age from an Antarctic ice core. *Nature*, *357*(6378), 488–490. https://doi.org/10.1038/357488a0

Levy, H., Moxim, W. J., Klonecki, A. A., & Kasibhatla, P. S. (1999). Simulated tropospheric NO_x: Its evaluation, global distribution and individual source contributions. *Journal of Geophysical Research*, *104*(D21), 26,279–26,306. https://doi.org/10.1029/1999JD900442

Li, J., Michalski, G., Davy, P., Harvey, M., Katzman, T., & Wilkins, B. (2018). Investigating source contributions of size-aggregated aerosols collected in Southern Ocean and Baring Head, New Zealand using sulfur isotopes. *Geophysical Research Letters*, *45*, 3717–3727. https://doi.org/10.1002/2018GL077353

Li, S.-M., & Barrie, L. A. (1993). Biogenic sulfur aerosol in the Arctic troposphere: 1. Contributions to total sulfate. *Journal of Geophysical Research*, *98*(D11), 20,613–20,622. https://doi.org/10.1029/93JD02234

Liang, J., & Jacobson, M. Z. (1999). A study of sulfur dioxide oxidation pathways over a range of liquid water contents, pH values, and temperatures. *Journal of Geophysical Research*, *104*(D11), 13,749–13,769. https://doi.org/10.1029/1999JD900097

Liotta, M., Rizzo, A., Paonita, A., Caracausi, A., & Martelli, M. (2012). Sulfur isotopic compositions of fumarolic and plume gases at Mount Etna (Italy) and inferences on their magmatic source. *Geochemistry, Geophysics, Geosystems*, *13*, Q05015. https://doi.org/10.1029/2012GC004118

Liu, Q., Schurter, L. M., Muller, C. E., Aloisio, S., Francisco, J. S., & Margerum, D. W. (2001). Kinetics and mechanisms of aqueous ozone reactions with bromide, sulfite, hydrogen sulfite, iodide, and nitrite ions. *Inorganic Chemistry*, *40*(17), 4436–4442. https://doi.org/10.1021/ic000919j

Lyons, J. R. (2001). Transfer of mass-independent fractionation in ozone to other oxygen-containing radicals in the atmosphere. *Geophysical Research Letters*, *28*(17), 3231–3234. https://doi.org/10.1029/2000GL012791

MacFarling Meure, C., Etheridge, D., Trudinger, C., Steele, P., Langenfelds, R., van Ommen, T., et al. (2006). Law Dome CO_2, CH_4 and N_2O ice core records extended to 2000 years BP. *Geophysical Research Letters*, *33*, L14810. https://doi.org/10.1029/2006GL026152

Mauldin, R. L., Eisele, F. L., Tanner, D. J., Kosciuch, E., Shetter, R., Lefer, B., et al. (2001). Measurements of OH, H_2SO_4, and MSA at the South Pole during ISCAT. *Geophysical Research Letters*, *28*(19), 3629–3632. https://doi.org/10.1029/2000GL012711

McCabe, J. R., Thiemens, M. H., & Savarino, J. (2007). A record of ozone variability in South Pole Antarctic snow: Role of nitrate oxygen isotopes. *Journal of Geophysical Research*, *112*, D12303. https://doi.org/10.1029/2006JD007822

Michalski, G., Bhattacharya, S. K., & Mase, D. F. (2012). Oxygen isotope dynamics of atmospheric nitrate and its precursor molecules. In *Handbook of environmental isotope geochemistry*, (pp. 613–635). Berlin, Heidelberg: Springer.

Michalski, G., Bockheim, J. G., Kendall, C., & Thiemens, M. (2005). Isotopic composition of Antarctic Dry Valley nitrate: Implications for NO_y sources and cycling in Antarctica. *Geophysical Research Letters*, *32*, L13817. https://doi.org/10.1029/2004GL022121

Michalski, G., Savarino, J., Böhlke, J. K., & Thiemens, M. (2002). Determination of the total oxygen isotopic composition of nitrate and the calibration of a $\Delta^{17}O$ nitrate reference material. *Analytical Chemistry*, *74*(19), 4989–4993. https://doi.org/10.1021/ac0256282

Michalski, G., Scott, Z., Kabiling, M., & Thiemens, M. H. (2003). First measurements and modeling of $\Delta^{17}O$ in atmospheric nitrate. *Geophysical Research Letters*, *30*(16), 1870. https://doi.org/10.1029/2003GL017015

Morin, S., Sander, R., & Savarino, J. (2011). Simulation of the diurnal variations of the oxygen isotope anomaly ($\Delta^{17}O$) of reactive atmospheric species. *Atmospheric Chemistry and Physics*, *11*(8), 3653–3671. https://doi.org/10.5194/acp-11-3653-2011

Morin, S., Savarino, J., Bekki, S., Gong, S., & Bottenheim, J. W. (2007). Signature of Arctic surface ozone depletion events in the isotope anomaly ($\Delta^{17}O$) of atmospheric nitrate. *Atmospheric Chemistry and Physics*, *7*(5), 1451–1469. https://doi.org/10.5194/acp-7-1451-2007

Morin, S., Savarino, J., Frey, M. M., Domine, F., Jacobi, H.-W., Kaleschke, L., & Martins, J. M. F. (2009). Comprehensive isotopic composition of atmospheric nitrate in the Atlantic Ocean boundary layer from 65°S to 79°N. *Journal of Geophysical Research*, *114*, D05303. https://doi.org/10.1029/2008JD010696

Morin, S., Savarino, J., Frey, M. M., Yan, N., Bekki, S., Bottenheim, J. W., & Martins, J. M. (2008). Tracing the origin and fate of NO_x in the Arctic atmosphere using stable isotopes in nitrate. *Science*, *322*(5902), 730–732. https://doi.org/10.1126/science.1161910

Nielsen, H. (1974). Isotopic composition of the major contributors to atmospheric sulfur. *Tellus*, *26*(1–2), 213–221.

Norman, A. L., Barrie, L. A., Toom-Sauntry, D., Sirois, A., Krouse, H. R., Li, S. M., & Sharma, S. (1999). Sources of aerosol sulphate at Alert: Apportionment using stable isotopes. *Journal of Geophysical Research*, *104*(D9), 11,619–11,631. https://doi.org/10.1029/1999JD900078

Pandis, S. N., & Seinfeld, J. H. (1989). Sensitivity analysis of a chemical mechanism for aqueous-phase atmospheric chemistry. *Journal of Geophysical Research*, *94*(D1), 1105–1126. https://doi.org/10.1029/JD094iD01p01105

Patris, N., Delmas, R., Legrand, M., De Angelis, M., Ferron, F. A., Stiévenard, M., & Jouzel, J. (2002). First sulfur isotope measurements in central Greenland ice cores along the preindustrial and industrial periods. *Journal of Geophysical Research*, *107*(D11), 4115. https://doi.org/10.1029/2001JD000672

Patris, N., Delmas, R. J., & Jouzel, J. (2000). Isotopic signatures of sulfur in shallow Antarctic ice cores. *Journal of Geophysical Research*, *105*(D6), 7071–7078. https://doi.org/10.1029/1999JD900974

Preunkert, S., Jourdain, B., Legrand, M., Udisti, R., Becagli, S., & Cerri, O. (2008). Seasonality of sulfur species (dimethyl sulfide, sulfate, and methanesulfonate) in Antarctica: Inland versus coastal regions. *Journal of Geophysical Research*, *113*, D15302. https://doi.org/10.1029/2008JD009937

Rees, C. E., Jenkins, W. J., & Monster, J. (1978). The sulphur isotopic composition of ocean water sulphate. *Geochimica et Cosmochimica Acta*, *42*(4), 377–381. https://doi.org/10.1016/0016-7037(78)90268-5

Röthlisberger, R., Hutterli, M. A., Sommer, S., Wolff, E. W., & Mulvaney, R. (2000). Factors controlling nitrate in ice cores: Evidence from the Dome C deep ice core. *Journal of Geophysical Research*, *105*(D16), 20,565–20,572. https://doi.org/10.1029/2000JD900264

Sanusi, A. A., Norman, A.-L., Burridge, C., Wadleigh, M., & Tang, W.-W. (2006). Determination of the S isotope composition of methanesulfonic acid. *Analytical Chemistry*, *78*(14), 4964–4968. https://doi.org/10.1021/ac0600048

21698996, 2019, 14, Downloaded from https://agupubs.onlinelibrary.wiley.com/doi/10.1029/2019JD030517 by Cochrane France, Wiley Online Library on [11/11/2024]. See the Terms and Conditions (https://onlinelibrary.wiley.com/terms-and-conditions) on Wiley Online Library for rules of use; OA articles are governed by the applicable Creative Commons License

Savarino, J., Alexander, B., Darmohusodo, V., & Thiemens, M. H. (2001). Sulfur and oxygen isotope analysis of sulfate at micromole levels using a pyrolysis technique in a continuous flow system. *Analytical Chemistry*, *73*(18), 4457–4462. https://doi.org/10.1021/ac010017f

Savarino, J., Bekki, S., Cole-Dai, J., & Thiemens, M. H. (2003). Evidence from sulfate mass independent oxygen isotopic compositions of dramatic changes in atmospheric oxidation following massive volcanic eruptions. *Journal of Geophysical Research*, *108*(D21), 4671. https://doi.org/10.1029/2003JD003737

Savarino, J., Kaiser, J., Morin, S., Sigman, D. M., & Thiemens, M. H. (2007). Nitrogen and oxygen isotopic constraints on the origin of atmospheric nitrate in coastal Antarctica. *Atmospheric Chemistry and Physics*, *7*(8), 1925–1945. https://doi.org/10.5194/acp-7-1925-2007

Savarino, J., Lee, C. C., & Thiemens, M. H. (2000). Laboratory oxygen isotopic study of sulfur (IV) oxidation: Origin of the mass-independent oxygen isotopic anomaly in atmospheric sulfates and sulfate mineral deposits on Earth. *Journal of Geophysical Research*, *105*(D23), 29,079–29,088. https://doi.org/10.1029/2000JD900456

Savarino, J., Morin, S., Erbland, J., Grannec, F., Patey, M. D., Vicars, W., et al. (2013). Isotopic composition of atmospheric nitrate in a tropical marine boundary layer. *Proceedings of the National Academy of Sciences*, *110*(44), 17,668–17,673. https://doi.org/10.1073/pnas.1216639110

Savarino, J., & Thiemens, M. H. (1999). Analytical procedure to determine both $\delta^{18}O$ and $\delta^{17}O$ of H_2O_2 in natural water and first measurements. *Atmospheric Environment*, *33*(22), 3683–3690. https://doi.org/10.1016/S1352-2310(99)00122-3

Savarino, J., Vicars, W. C., Legrand, M., Preunkert, S., Jourdain, B., Frey, M. M., et al. (2016). Oxygen isotope mass balance of atmospheric nitrate at Dome C, East Antarctica, during the OPALE campaign. *Atmospheric Chemistry and Physics*, *16*(4), 2659–2673. https://doi.org/10.5194/acp-16-2659-2016

Shaheen, R., Abauanza, M., Jackson, T. L., McCabe, J., Savarino, J., & Thiemens, M. H. (2013). Tales of volcanoes and El-Niño southern oscillations with the oxygen isotope anomaly of sulfate aerosol. *Proceedings of the National Academy of Sciences*, *110*(44), 17662–17667. https://doi.org/10.1073/pnas.1213149110

Shaw, G. E. (1988). Antarctic aerosols: A review. *Reviews of Geophysics*, *26*, 89–112. https://doi.org/10.1029/RG026i001p00089

Stein, A. F., Draxler, R. R., Rolph, G. D., Stunder, B. J., Cohen, M. D., & Ngan, F. (2015). NOAA's HYSPLIT atmospheric transport and dispersion modeling system. *Bulletin of the American Meteorological Society*, *96*(12), 2059–2077. https://doi.org/10.1175/BAMS-D-14-00110.1

Stohl, A., & Sodemann, H. (2010). Characteristics of atmospheric transport into the Antarctic troposphere. *Journal of Geophysical Research*, *115*, D02305. https://doi.org/10.1029/2009JD012536

Troy, R. C., & Margerum, D. W. (1991). Non-metal redox kinetics: Hypobromite and hypobromous acid reactions with iodide and with sulfite and the hydrolysis of bromosulfate. *Inorganic Chemistry*, *30*(18), 3538–3543. https://doi.org/10.1021/ic00018a028

Varotsos, C. (2002). The southern hemisphere ozone hole split in 2002. *Environmental Science and Pollution Research*, *9*(6), 375–376. https://doi.org/10.1007/BF02987584

Vicars, W. C., Bhattacharya, S. K., Erbland, J., & Savarino, J. (2012). Measurement of the ^{17}O-excess ($\Delta^{17}O$) of tropospheric ozone using a nitrite-coated filter. *Rapid Communications in Mass Spectrometry*, *26*(10), 1219–1231. https://doi.org/10.1002/rcm.6218

Vicars, W. C., & Savarino, J. (2014). Quantitative constraints on the ^{17} O-excess ($\Delta^{17}O$) signature of surface ozone: Ambient measurements from 50° N to 50° S using the nitrite-coated filter technique. *Geochimica et Cosmochimica Acta*, *135*, 270–287. https://doi.org/10.1016/j.gca.2014.03.023

Wagenbach, D. (1996). Coastal Antarctica: Atmospheric chemical composition and atmospheric transport. In *Chemical exchange between the atmosphere and polar snow*, (pp. 173–199). Berlin, Heidelberg: Springer.

Weller, R., Legrand, M., & Preunkert, S. (2018). Size distribution and ionic composition of marine summer aerosol at the continental Antarctic site Kohnen. *Atmospheric Chemistry and Physics*, *18*(4), 2413–2430. https://doi.org/10.5194/acp-18-2413-2018

Wendler, G., & Kodama, Y. (1984). On the climate of Dome C, Antarctica, in relation to its geographical setting. *International Journal of Climatology*, *4*(5), 495–508. https://doi.org/10.1002/joc.3370040505

Weston, R. E. Jr. (2006). When is an isotope effect non-mass dependent. *Journal of Nuclear Science and Technology*, *43*(4), 295–299. https://doi.org/10.1080/18811248.2006.9711092

Young, E. D., Galy, A., & Nagahara, H. (2002). Kinetic and equilibrium mass-dependent isotope fractionation laws in nature and their geochemical and cosmochemical significance. *Geochimica et Cosmochimica Acta*, *66*(6), 1095–1104. https://doi.org/10.1016/S0016-7037(01)00832-8

21698996, 2019, 14, Downloaded from https://agupubs.onlinelibrary.wiley.com/doi/10.1029/2019JD030517 by Cochrane France, Wiley Online Library on [11/11/2024]. See the Terms and Conditions (https://onlinelibrary.wiley.com/terms-and-conditions) on Wiley Online Library for rules of use; OA articles are governed by the applicable Creative Commons License